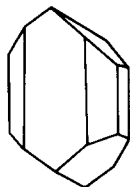# Compositional variations among gabbroic intrusions in the Oslo rift

ELSE-RAGNHILD NEUMANN, BJØRN T. LARSEN and BJØRN SUNDVOLL

Mineralogisk-Geologisk Museum, Sarsgt. 1, Oslo (Norway)

LITHOS

Magmatic activity associated with the formation of the Oslo rift, South Norway, in Permo-Carboniferous time includes formation of a series of gabbroic intrusions of minor volume. The rock types in these intrusions range from pyroxenite and gabbro to monzonite and anorthosite. The mafic units bear evidence of the crystallization order ol → cpx → ±opx → plag, whereas the more evolved rock types have crystallized olivine and plagioclase before clinopyroxene. Amphibole occasionally represents an early phase. Major and trace element data imply that removal of clinopyroxene has dominated the early crystallization history of all these rocks, this is also true for rocks which give petrographic evidence of crystallization of cpx *after* plag. Rb-Sr isotope data define a whole rock age of 265 ± 11 for the Snaukollen and a mineral age of 266 ± 5 Ma for the Dignes intrusion. Whole rock samples from the other intrusions, however, do not define isochrons but cover a range of $^{87}Sr/^{86}Sr$ ratios from 0.70395 to 0.71187.

It is concluded that the gabbroic Oslo rift rocks are produced through a two-stage crystallization history combined with crustal contamination:

(1) Mafic magmas ascending from some melt region in the mantle were retained in the lower crust where they crystallized olivine and clinopyroxene.

(2) At different stages of evolution residual magmas rose to their present position in the upper crust. Depending on composition, the crystallization sequence there was ol → cpx → plag or ol → plag → cpx.

(3) During the final stage of evolution the magmas were to different degrees contaminated by Precambrian amphibolite facies and Cambro-Silurian carbonaceous country rock. Early crystallization of amphibole combined with interstitial calcite in some rocks, and highly variable Fe^{3+} contents in clinopyroxene imply significant variations in the volatile phase of the magmas which gave rise to the gabbroic rocks. These differences may have been introduced through the contamination. However, the possibility of primary compositional contrasts cannot be excluded.

Introduction

The Oslo Region mildly alkaline province formed in the Permo-Carboniferous period through an intracontinental rifting episode accompanied by extensive magmatism (Fig. 1). The magmatic activity started about 304 Ma ago with eruptions mainly of basalts and rhomb porphyry lavas from fissures, later from central volcanoes, and terminated with the emplacement of large intermediate to silicic batholiths, the youngest of which is 245 Ma old (Ramberg and Larsen, 1978; Sundvoll, 1978a).

Basic intrusions of minor volume also occur in the Oslo rift. Fifteen small bodies are known, six of which are double or triple, plus some very small occurrences (Fig. 1). The basic plutonic rocks were first described by Brøgger (1894, 1931, 1933a, b). Initially he called them gabbrodiabase and basic eruptive rocks, but later (1931) he classified them as essexites although they do not contain nepheline. In an attempt to remedy this inconsistency, Barth (1945) introduced the name "Oslo-essexite", which has since been used in the literature. A suggestion to reclassification is discussed below.

36
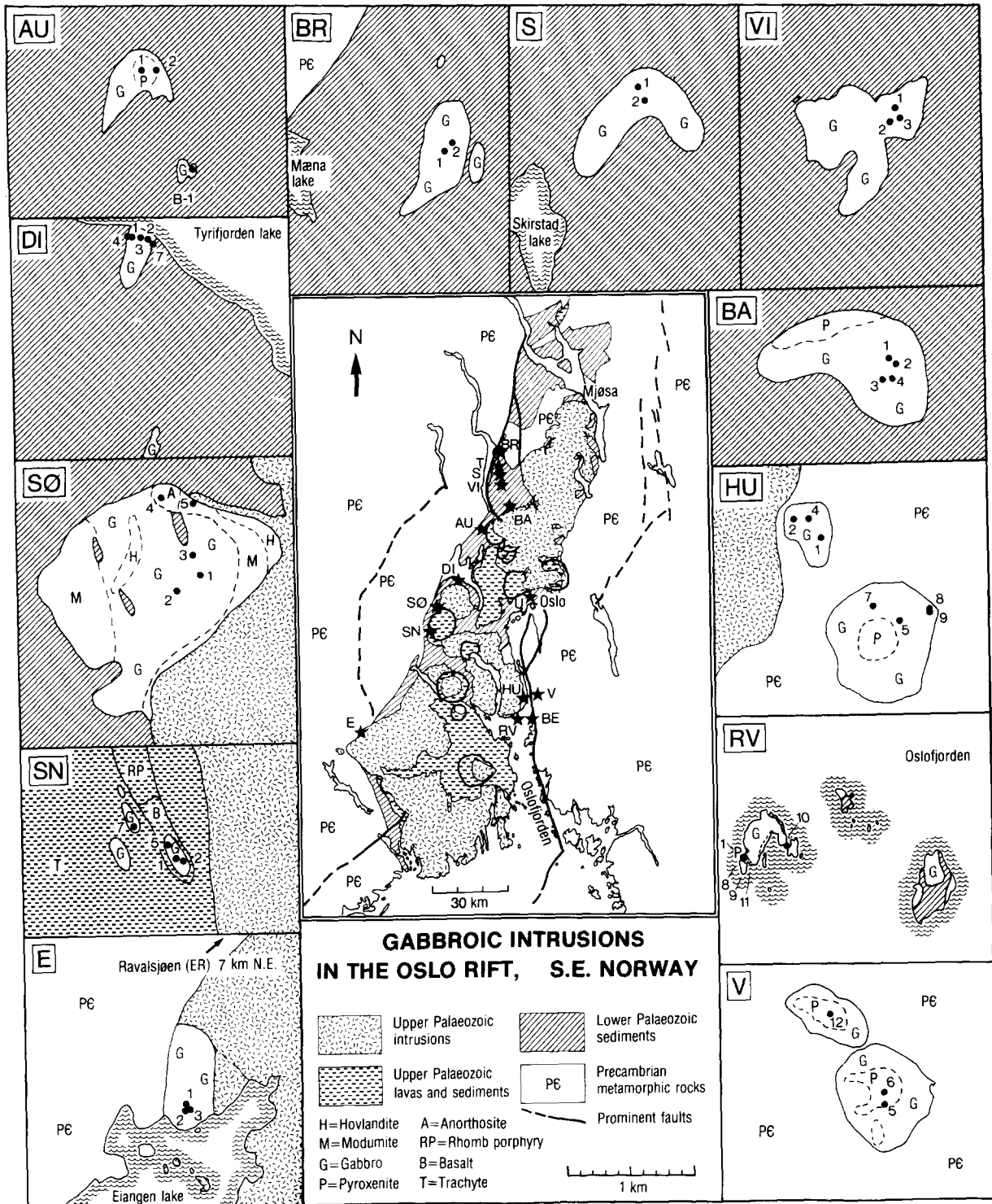
Fig. 1. The central diagram is a generalized geological map of the Oslo rift showing the locations of the gabbroic intrusions. The surrounding maps show rock types and sample localities in the bodies described in this paper. Data are from Brøgger (1933), Barth (1945), Ramberg (1970) and the present authors. Hovlandite = syenogabbro occurring as a borderfacies between modumite and granite. Modumite = anorthosite of bytownitic composition bearing hornblende or biotite. Abbreviations: BR = Brandbu-kampen, T = Tingelstad, S = Sølvsberget, VI = Viksberget, BA = Ballangrudkollen, U = Ullernåsen, HU = Husebykollen, RV = Ramvikholmen, V = Vestby, AU = Aurenhøgda, DI = Dignes, SØ = Sønstebyflakene, SN = Snaukollen, E = Eiangen (BE = Bevøy).

The position of the small mafic plutons in the evolutionary history of the Oslo rift, and their genetic relationship to the lavas and felsic batholiths, are still uncertain. It was first proposed that they belong to the earliest magmatic activity in the rift (Brøgger, 1933a). A more recent view is that they formed during the stage of central volcanism and cauldron subsidence and may represent feeders to volcanoes (B_3) (Dons, 1952; Oftedahl, 1952, 1953; Ramberg and Larsen, 1978).

Prior to the present study, reliable compositional data on the mafic intrusive rocks were limited. Isotopic analyses and systematic mineralogical investigations had never been undertaken.

We consider the mafic intrusions, although small in volume, to be important to the understanding of the tectonomagmatic evolution of the Oslo rift: They comprise the only mafic intrusive rocks in the rift; they are distinctively small compared to the other intrusive complexes; and their geographic distribution suggests a strong tectonic control. The present geochemical survey of these rocks was undertaken in order to (1) define their compositional characteristics and possible regional variations, (2) test their genetic relationship to the various mafic lava groups, and (3) throw some light on their petrogenetic history.

Supplementing the present survey study a detailed geological, petrological and geochemical investigation was conducted on the well exposed Husebykollen and Ramvikholmen bodies (described in a thesis by Steinlein, 1981). This will be published separately.

Geology

The small mafic plutons are distributed along two lines, one N-S, the other NNE-SSW, parallel to the two major fault trends in the Oslo rift (Brøgger, 1933b) (Fig. 1). Most of the bodies intrude the lower Palaeozoic sediments and Precambrian basement exposed along the rift margins. The Snaukollen (SN) body dissects basalts of the central volcano stage (B_3), whereas two adjacent basic bodies occur as huge xenoliths in the syenite porphyry ring-dyke of a cauldron (Oftedahl, 1952) (Fig. 1). Also other small bodies of gabbroic rocks appear to be megaxenoliths in the felsic intrusions (Ramberg, 1976; Larsen et al., 1978; E. Rasmussen, personal communication, 1981).

The intrusions are 0.3 to about 3 km in diameter. The largest one is the Sønstebyflakene (SØ), the smallest one the Bevøy (BE) body (Fig. 1). The bodies are roughly circular, except for the Viksbergene (VI) intrusion which may be a composite of two or three intrusions. The vertical extent of the plutons below the present erosion surface seems to be small, gravity data suggest thicknesses of only 0.5–1.5 km, with each mafic body having a thickness smaller than, or similar to its average diameter (Ramberg, 1976).

The plutons are composed of a range of rock types which have been presented in the literature under a variety of exotic names. According to Streckeisen's (1976) classification system the main rock types are fine- to coarse-grained gabbro, diorite, monzodiorite, monzogabbro, monzonite, pyroxenite, olivine-pyroxenite and anorthosite. Some rocks contain amphibole instead of pyroxene. Cumulate textures are common. In many intrusions the rock units are concentrically arranged (Fig. 1), the most felsic rocks are found both in the center (e.g., Ullernåsen (U)) and along the rim (e.g., Husebykollen (HU), Vestby (V)) (Brøgger, 1931; Dons, 1952; Ramberg, 1970; Steinlein, 1981). Rhythmic layering can be seen in most of the bodies. The layers dip steeply and are a few centimeters to several meters thick (Larsen et al., 1978). Erosion channels, angular unconformities between layers and rock units, and slumps, suggest the erosional effect of convection currents in unconsolidated cumulates. Cumulate textures and structures are best exposed at Ramvikholmen (RV), and are described and discussed in detail by Steinlein (1981).

McCulloh (1952) has estimated that the present erosion surface in the Oslo Region is about 3 km lower than in Permian time. Thus, if Ramberg's (1976) estimate that the gabbro intrusions extend only to depths between 0.3 and 1.5 km below the present level of erosion is valid, the bodies have crystallized at low pressures, probably as floored subvolcanic magma chambers.

Petrography

Representative samples of the different rock types in the mafic intrusions have been selected for analyses. These rocks are described below.

The *Brandbukampen* (BR) rocks BR-1 and BR-2D consist primarily of subhedral, zoned clinopyroxene (diameter <10 mm) in patchy intergrowth with kaersutite. Interstitial phases are Ti-rich amphibole, Fe-Ti oxides, calcite, apatite and sphene. BR-2A has

phenocrysts of olivine (diameter <3 mm) and strongly zoned clinopyroxene (diameter ⩽6 mm) with some grains displaying hourglass-zoning. Olivine and oxides occur as inclusions in clinopyroxene phenocrysts. The groundmass is fine-grained plagioclase, olivine, clinopyroxene, apatite and Fe-Ti oxides. BR-2B is a somewhat altered hornblende-clinopyroxene gabbro rich in apatite and sphene, secondary biotite and amphibole. BR-KF consists of about 30% (modal) zoned plagioclase (An$_{54}$), 30% clinopyroxene, alkali feldspar, apatite, Fe-Ti oxides, and biotite (Finstad, 1972).

The *Tingelstad* (T) sample analyzed by Finstad (1972) consists of about 55% (modal) zoned plagioclase (An$_{54}$), 28% Ti-rich amphibole, alkali feldspar, apatite and Fe-Ti oxides.

The *Sølvsberget* (S) sample S-1 is a medium-grained (diameter ⩽2 mm) olivine gabbro consisting primarily of mildly zoned plagioclase plus unzoned olivine, zoned clinopyroxene, Fe-Ti oxides and apatite. Olivine, plagioclase and oxides are found as inclusions in clinopyroxene. Sample S-KF consists of 70% (modal) plagioclase (An$_{44}$) and alkali feldspar, olivine, augite, biotite and Fe-Ti oxides (Finstad, 1972).

The *Viksberget* (VI) samples are feldspathic olivine gabbros consisting of up to 4 mm long grains of subhedral olivine, sub- to anhedral zoned plagioclase, sub- to anhedral, poikilitic, zoned clinopyroxene, Fe-Ti oxides and apatite. Clinopyroxene has inclusions of all the other phases. Minor alteration of plagioclase to sericite and mafic silicates to biotite may be observed. VI-KF has minor amounts of calcite.

Also the *Ballangrudkollen* (BA) rocks are feldspathic gabbros. Phenocrysts of subhedral olivine (diameter ⩽5 mm), zoned, subhedral clinopyroxene (⩽5 mm), and scattered microphenocrysts of zoned plagioclase lie in a groundmass of plagioclase with some oxides, clinopyroxene, apatite and alkali feldspar. Olivine, oxides and plagioclase are found as inclusions in clinopyroxene phenocrysts, particularly near the rim. Traces of orthopyroxene have been observed as reaction rims on olivine. Samples BA-1, 2, and 3 have minor amounts of secondary biotite, chlorite, chrysotile and sericite. BA-4 is strongly altered with complete breakdown of olivine to oxide + chlorite, and partial replacement of clinopyroxene by amphibole, biotite and chlorite.

The *Ullernåsen-Husebyåsen* (Bærum) (U) samples are described by Dons (1952).

The analyzed *Husebykollen* (HU) samples HU-1 to HU-4 are from the small body, samples HU-5 to HU-9 are from the main body. HU-1, 4, 5 and 8 are olivine-clinopyroxenites, exhibiting a framework of up to 10 mm long, euhedral, strongly zoned clinopyroxenes and minor amounts of smaller olivine phenocrysts, with interstitial plagioclase, Fe-Ti oxides, apatite and calcite. Olivine and oxides occur as inclusions in clinopyroxene. HU-2, 7, and 9 have moderate amounts of clinopyroxene and olivine-phenocrysts in a similar groundmass. Samples HU-5, and 8 are fairly fresh, HU-1 to 4 and HU-7 and 9 are strongly altered with secondary biotite, chlorite, sericite, Fe-Ti oxides and quartz.

The *Ramvikholmen* (RV) intrusions comprises a variety of rock types which are described by Steinlein (1981).

The samples from the two small intrusions at *Vestby* (V) are described by Ramberg (1970). V-KF, V-IR2 and V-IR4 are made up by 90–95% (modal) zoned clinopyroxene, together with olivine and olivine pseudomorphs, Fe-Ti oxides, apatite and scattered grains of plagioclase, kaersutite and calcite. V-IR3 and V-IR5 consist of more than 50% (modal) strongly sericitized, euhedral plagioclase, some pseudomorphs after olivine, euhedral alkali feldspar, somewhat altered clinopyroxene, hornblende, Fe-Ti oxides, apatite, rutile, sphene and secondary biotite, often associated with oxides, and chlorite. Neither quartz nor nepheline have been observed in these rocks.

Also the *Aurenhøgda* (AU) samples AU-1 and AU-2 are olivine-clinopyroxenites, with up to 20 mm long pyroxene phenocrysts. Interstitial phases are minor amounts of plagioclase + Fe-Ti oxides + apatite + calcite. AU-2 also has kaersutite both intergrown with clinopyroxene, and as an interstitial phase. Olivine is partly broken down to chlorite + oxides. AU-KF is monzodiorite: 70% modal plagioclase (An$_{38}$) and alkalifeldspar, about 25% clinopyroxene, Fe-Ti oxides, apatite and biotite (Finstad, 1972). AU-B1 from the twin plug is a coarse-grained gabbro consisting mainly of zoned plagioclase crystals with interlocking boundaries and subhedral poikilitic grains of clinopyroxene with interlocking boundaries and inclusions of plagioclase, oxides and apatite. The rock contains calcite and is relatively rich in apatite and oxide. Some secondary biotite, chlorite and sericite are found.

The *Dignes* (DI) rocks have phenocrysts of sub-

hedral, weakly zoned plagioclase (up to 5 mm long) and minor amounts of olivine (up to 2 mm in diameter) in a groundmass of clinopyroxene, apatite, Fe-Ti oxides and alkali feldspar. The analyzed samples contain minor amounts of secondary biotite and sericite.

The *Sønstebyflakene* (SØ) samples fall into two textural groups. SØ-1, 2 and 3 are fine-grained monzodiorites with subhedral zoned plagioclase, remnants of clinopyroxene in subhedral grains of brownish to greenish hornblende which is partly altered to biotite and chlorite, considerable amounts of quartz, partly as rounded grains, partly in complex intergrowth with strongly sericitized feldspar, alkali feldspar, sphene, oxides, apatite and calcite. SØ-4 is porphyritic with a framework of plagioclase phenocrysts (up to 20 mm long) in a groundmass of clinopyroxene, plagioclase, oxides and considerable amounts of quartz and apatite. The rock is considerably altered with secondary chlorite and sericite. SØ-5 is similar to SØ-4, but only has traces of clinopyroxene in subhedral grains of dark brown kaersutite partly altered to biotite and chlorite, and it contains calcite. Aggregates of chlorite and oxides appear to be pseudomorphs after olivine.

In the *Snaukollen* (SN) rocks up to 20 mm long, subhedral, zoned plagioclase crystals form a framework with clinopyroxene, considerable amounts of Fe-Ti oxides, fine-grained quartz, apatite and alkali-feldspar in the interstices. SN-2 and SN-5 also have phenocrysts of (or pseudomorphs after) olivine, and no quartz. With the exception of sample SN-2 these rocks are somewhat altered, with secondary growth of biotite, chlorite and sericite.

The *Eiangen* (E) samples E-1, 2 and 3 are feldspathic gabbros consisting of subhedral olivine (or olivine pseudomorphs) and plagioclase, subhedral to anhedral clinopyroxene and orthopyroxene, alkali feldspar, very minor amounts of apatite and Fe-Ti oxides, and some secondary biotite and chlorite. Olivine is frequently enclosed by pyroxene. E-1 and E-3 are rich in olivine. The two analyzed samples from the twin-pluton at *Ravalsjøen* (E-4 and E-5) consist mainly of strongly zoned clinopyroxene, up to 6 mm long, intergrown with kaersutite, and with exsolved Fe-Ti oxides along structural planes. The groundmass is subhedral fresh clinopyroxene and brown amphibole, anhedral strongly sericitized plagioclase, oxides, sphene, biotite, chlorite and calcite. The described textures suggest that some of the

rocks of this study are cumulates (as defined by Irvine, 1982), whereas others may have compositions close to those of the melts from which they formed. Both phenocrysts and cumulus crystals represent early-formed phases in a magma, and thus provide an important basis for defining patterns of mineral fractionation. The different phenocryst/cumulus crystal assemblages found among the Oslo rift mafic intrusive rocks appear to reflect genetically significant differences in the crystallization order of the major silicates (abbreviations as above):

(a) ol, cpx   (S, BA, U, HU, RV, V, AU)
(b) ol, cpx + amph (BR, U, E)
(c) ol, cpx + plag (VI)
(d) ol + plag   (S, U, RV, AU, DI, SN, E)
(e) plag, ol   (RV)
(f) amph   (BR, T, U, HU, RV, SØ)

Fe-Ti oxides have crystallized early in each case.

The above list of crystallization orders is based on the extensive thin-section study made during the present investigation, plus descriptions given by Brøgger (1931), Dons (1952), Ramberg (1970) and Steinlein (1981).

Early crystallization of kaersutitic amphibole (crystallization order b and f) is mainly restricted to calcite-bearing rocks (BR, HU, V, AU, SØ).

Mineral compositions

Olivine, pyroxene, amphibole and plagioclase in selected rocks were analyzed on an ARL-EMX electron microprobe equipped with a LINK energy-dispersive detector system.

Olivine

The analyzed olivines range in composition from Fo_{79} to Fo_{38}. Individual crystals frequently are slightly zoned. In a number of these rocks olivine is partly or totally broken down to alteration products. In spite of the textural indications that olivine has crystallized before, or simultaneously with, clinopyroxene in these rocks, olivine is frequently considerably less magnesian than coexisting clinopyroxene. Experimental data on ol-liquid and cpx-liquid equilibria, suggest the following exchange reaction (Navrotsky, 1978):

TABLE 1

Representative analyses of pyroxenes, with structural formulae calculated on the basis of 4.000 cations. Fe^{3+} has been calculated from charge balance. Samples with both Ca-rich and Ca-poor pyroxene are marked cp + op, other samples only have Ca-rich pyroxene

	BR-2B		BR-2D		S-1		VI-3A	Ba-2 (cp+up)			HU-6	HU-8	RV-11 (cp+op)		AU-2		
	PH		PH		PH		GR	PH		GR	PH	PH	PH		GR	PH	
	C	R	C	R	C	R	mean	C	R	trace		mean	C	R		C	R
SiO_2	48.07	49.20	49.04	45.18	51.14	51.10	49.82	48.26	49.99	52.41	51.63	49.39	53.04	50.76	52.57	52.18	49.80
TiO_2	1.67	1.00	1.79	3.17	0.96	0.73	1.60	1.63	1.43	0.19	1.26	1.57	0.54	1.16	0.19	0.57	1.74
Al_2O_3	4.35	3.37	5.50	6.60	2.64	1.91	3.57	5.00	2.67	0.66	2.44	3.26	1.40	2.13	0.48	2.72	4.44
Cr_2O_3	0.11	0.07	0.15	0.02	0.17	0.06	0.00	0.17	0.06	0.00			0.57	0.04	0.00	0.59	0.01
FeO_T	10.53	9.72	6.82	8.24	9.60	11.23	8.90	7.97	9.41	22.09	10.12	8.88	4.94	10.24	24.59	5.12	7.18
MnO	0.23	0.18	0.18	0.25	0.24	0.34	0.34	0.15	0.28	0.81	0.37	0.25	0.05	0.24	0.70	0.23	0.13
MgO	11.29	11.58	14.31	12.44	13.91	13.91	14.12	13.94	14.01	23.05	14.39	13.98	16.98	14.02	20.76	16.68	14.57
CaO	22.54	22.66	23.24	22.84	21.91	20.52	20.74	21.56	20.94	0.93	19.22	20.36	22.28	20.83	1.48	21.67	22.53
Na_2O	1.22	1.35	0.32	0.44	0.53	0.57	0.45	0.59	0.73	0.00	0.35	0.42	0.53	0.56	0.00	0.39	0.32
Total	100.02	99.15	101.20	99.16	100.71	100.37	99.54	99.29	99.52	100.14	99.78	98.37	99.76	99.94	100.77	100.15	100.79
Si	1.799	1.849	1.788	1.700	1.884	1.902	1.860	1.798	1.867	1.944	1.931	1.871	1.930	1.894	1.966	1.904	1.827
Al^{IV}	0.192	0.149	0.212	0.293	0.115	0.084	0.140	0.202	0.118	0.029	0.069	0.129	0.060	0.094	0.021	0.096	0.173
Al^{VI}	0.000	0.000	0.025	0.000	0.000	0.000	0.018	0.018	0.000	0.000	0.039	0.016	0.000	0.000	0.000	0.021	0.019
Ti	0.040	0.028	0.049	0.090	0.026	0.020	0.045	0.046	0.040	0.005	0.035	0.045	0.015	0.032	0.005	0.016	0.048
Cr	0.003	0.002	0.004	0.000	0.005	0.002	0.000	0.005	0.002	0.000			0.016	0.001	0.000	0.017	0.000
Fe^{3+}	0.020	0.019	0.107	0.160	0.010	0.011	0.065	0.013	0.012	0.007	0.000	0.057	0.013	0.009	0.004	0.005	0.008
Mg	0.630	0.649	0.778	0.698	0.764	0.772	0.786	0.774	0.780	1.274	0.802	0.789	0.921	0.780	1.157	0.907	0.797
Fe^{2+}	0.310	0.286	0.101	0.099	0.286	0.339	0.213	0.235	0.282	0.678	0.317	0.224	0.137	0.311	0.765	0.151	0.212
Mn	0.007	0.006	0.006	0.008	0.007	0.011	0.011	0.005	0.009	0.025	0.012	0.008	0.002	0.008	0.022	0.007	0.004
Ca	0.904	0.912	0.908	0.921	0.865	0.818	0.830	0.861	0.838	0.037	0.770	0.826	0.869	0.833	0.059	0.847	0.886
Na	0.089	0.098	0.023	0.032	0.038	0.041	0.033	0.043	0.053	0.000	0.025	0.031	0.038	0.041	0.000	0.028	0.023

Abbreviations: PH = phenocrysts, GR = interstitial, C = core, R = rim.

TABLE 1 (continued)

	D-2	D-3		D-4A	D-7	SØ-2	SØ-4	SN-2	SN-7	E-1 (cp+op)		ER-5		
	GR	GR C	GR R	GR mean	GR	mean	GR mean	GR mean	GR mean	GR	GR	PH C	PH R	GR
SiO_2	48.45	50.55	49.74	51.08	50.08	52.25	50.29	49.67	49.61	49.52	54.25	52.63	49.60	53.59
TiO_2	1.31	0.88	0.91	1.23	1.38	0.30	0.98	1.35	1.20	1.52	0.24	0.75	1.29	0.22
Al_2O_3	3.26	2.81	2.90	2.02	2.07	1.38	1.12	3.48	1.50	3.63	1.00	2.43	3.16	0.90
Cr_2O_3	0.02			0.00	0.09		0.06	0.00	0.06	0.12	0.07	0.25	0.19	0.01
FeO_T	14.99	10.97	13.01	10.75	11.52	8.27	16.75	7.70	15.06	7.35	15.53	4.68	7.57	5.05
MnO	0.36	0.28	0.32	0.33	0.17	0.47	0.75	0.19	0.34	0.12	0.42	0.15	0.40	0.26
MgO	7.99	11.34	9.76	13.18	11.61	14.81	10.77	14.90	11.71	15.03	27.61	15.86	14.07	14.81
CaO	21.71	22.40	22.16	21.26	21.84	21.70	19.23	21.65	19.58	21.42	1.10	22.32	19.95	23.25
Na_2O	1.30	1.09	1.03	0.93	1.04	0.35	0.32	0.58	0.55	0.50	0.00	0.62	1.07	0.60
Total	99.39	100.32	99.83	100.78	99.80	99.53	100.27	99.52	99.61	99.21	100.22	99.44	97.11	99.13
Si	1.867	1.891	1.890	1.900	1.888	1.946	1.928	1.841	1.895	1.841	1.949	1.930	1.880	1.989
AlIV	0.133	0.109	0.110	0.088	0.092	0.054	0.051	0.152	0.068	0.159	0.042	0.070	0.120	0.011
AlVI	0.015	0.014	0.020	0.000	0.000	0.006	0.000	0.000	0.000	0.000	0.000	0.035	0.021	0.028
Ti	0.038	0.025	0.026	0.035	0.040	0.008	0.028	0.038	0.034	0.042	0.006	0.021	0.037	0.006
Cr	0.001			0.000	0.003		0.02	0.000	0.002	0.004	0.002	0.007	0.006	0.000
Fe^{3+}	0.014	0.125	0.114	0.121	0.013	0.056	0.058	0.013	0.011	0.011	0.004	0.030	0.098	0.014
Mg	0.459	0.632	0.553	0.729	0.652	0.822	0.616	0.823	0.667	0.833	1.478	0.867	0.795	0.819
Fe^{2+}	0.469	0.219	0.299	0.212	0.350	0.201	0.479	0.226	0.470	0.217	0.463	0.114	0.142	0.157
Mn	0.012	0.009	0.010	0.010	0.005	0.015	0.024	0.006	0.011	0.004	0.013	0.005	0.013	0.008
Ca	0.896	0.898	0.902	0.845	0.882	0.866	0.790	0.860	0.801	0.853	0.042	0.877	0.810	0.924
Na	0.097	0.079	0.076	0.067	0.076	0.025	0.024	0.042	0.041	0.036	0.000	0.044	0.879	0.043

TABLE 2

Representative analyses of amphiboles, with structural formulae calculated on the assumption that $(Si+Al+Ti+Mg+Fe+\frac{1}{2}Mn) = 13.000$ cations

	BR-1	BR-2B		BR-2D			BA-4C				SØ-1	
	INT	PH		INT			INT	RPX	RPX			
	mean	C	R	C	—	R			C	R	C	R
SiO_2	38.92	38.85	39.90	38.41	49.53	52.04	41.40	41.35	46.61	51.14	45.94	51.35
TiO_2	5.45	5.95	4.65	5.89	0.50	0.15	5.01	4.43	0.12	0.32	2.42	0.81
Al_2O_3	13.42	14.14	11.71	13.78	8.94	4.52	11.02	11.65	5.89	3.44	7.93	3.77
Cr_2O_3		0.00	0.20	0.02	0.00	0.00	0.09	0.05	0.11	0.00	0.00	0.00
FeO_T	11.49	10.43	14.27	10.67	6.77	7.94	12.32	13.49	25.09	16.51	12.13	10.90
MnO	0.25	0.00	0.34	0.17	0.11	0.12	0.34	0.22	0.17	0.25	0.39	0.42
MgO	11.67	12.87	11.08	12.93	18.64	19.09	12.57	12.80	7.33	12.85	14.80	17.20
CaO	11.76	12.50	11.74	12.32	13.21	13.24	11.53	11.71	12.19	12.36	11.03	11.54
Na_2O	2.55	2.50	2.68	2.35	0.71	0.35	2.26	2.46	0.57	0.60	2.00	1.03
K_2O	1.37	1.35	1.89	1.42	0.25	0.43	1.19	1.12	0.81	0.28	0.72	0.42
Total	96.88	98.59	98.46	97.96	98.66	97.88	97.73	99.28	98.89	97.75	97.36	97.44
Si	5.887	5.746	6.035	5.716	6.850	7.300	6.157	6.048	7.070	7.512	6.762	7.309
Al^{IV}	2.113	2.254	1.965	2.284	1.150	0.700	1.843	1.952	0.930	0.488	1.238	0.632
Al^{VI}	0.280	0.211	0.132	0.134	0.307	0.047	0.087	0.055	0.122	0.108	0.119	0.000
Ti	0.620	0.662	0.529	0.659	0.052	0.016	0.561	0.486	0.014	0.035	0.265	0.087
Cr		0.000	0.024	0.002	0.000	0.000	0.011	0.005	0.013	0.000	0.000	0.000
Mg	2.631	2.837	2.497	2.869	3.842	3.993	2.786	2.787	1.657	2.814	3.204	3.649
Fe_T	1.453	1.290	1.805	1.328	0.783	0.932	1.532	1.653	3.183	2.028	1.474	1.298
Mn	0.032	0.000	0.043	0.021	0.013	0.014	0.043	0.027	0.022	0.031	0.048	0.050
Ca	1.906	1.981	1.902	1.966	1.957	1.990	1.837	1.834	1.981	1.945	1.716	1.760
Na	0.748	0.717	0.786	0.678	0.190	0.095	0.652	0.697	0.167	0.170	0.564	0.284
K	0.264	0.255	0.365	0.269	0.044	0.077	0.226	0.209	0.156	0.053	0.133	0.076
A-site	0.934	0.953	1.075	0.923	0.197	0.169	0.736	0.753	0.315	0.184	0.437	0.145

	SØ-2	SØ-3	SØ-4		SØ-5	SØ-6		AU-2	ER-4	ER-5	
			GR1	GR2	PH	PH	GR	INT RPX	INT	PH	GR
	mean	mean			mean						
SiO_2	45.96	45.31	44.71	51.07	42.06	37.25	37.94	40.59	41.91	37.31	42.36
TiO_2	2.58	2.57	0.34	0.28	4.85	4.99	4.91	5.58	4.96	6.51	4.12
Al_2O_3	7.92	8.63	4.59	0.91	11.24	15.92	15.28	11.74	10.82	14.15	10.93
Cr_2O_3	0.00	0.00	0.04	0.05	0.03	0.04	0.05	0.19	0.03	0.02	0.04
FeO_T	12.42	12.06	28.88	23.19	11.00	13.84	12.56	10.70	10.92	11.21	10.58
MnO	0.37	0.42	1.56	1.13	0.31	0.36	0.34	0.13	0.28	0.08	0.23
MgO	14.78	15.09	6.90	8.84	14.19	11.43	12.57	13.45	13.28	16.39	13.59
CaO	11.05	11.11	9.11	10.90	11.16	11.58	11.55	11.94	11.44	11.30	11.51
Na_2O	1.91	2.13	1.17	0.30	2.94	2.43	2.51	2.74	2.87	3.21	3.15
K_2O	0.70	0.72	0.95	0.32	0.67	1.39	1.34	0.97	1.11	0.99	1.04
Total	97.69	98.04	98.25	96.99	98.45	99.24	99.05	98.03	97.62	101.17	97.55
Si	6.654	6.534	6.799	7.771	6.112	5.470	5.538	6.008	6.230	5.229	6.290
Al^{IV}	1.343	1.467	0.823	0.164	1.888	2.530	2.462	1.992	1.770	2.338	1.710
Al^{IV}	0.007	0.000	0.000	0.000	0.037	0.225	0.166	0.052	0.126	0.000	0.202
Ti	0.281	0.278	0.038	0.032	0.530	0.551	0.538	0.621	0.554	0.686	0.460
Cr	0.000	0.000	0.005	0.006	0.003	0.005	0.006	0.022	0.004	0.002	0.004
Mg	3.189	3.244	1.564	2.005	3.073	2.502	2.735	2.967	2.942	3.424	3.006
Fe_T	1.504	1.455	3.673	2.951	1.337	1.699	1.533	1.325	1.357	1.314	1.314
Mn	0.045	0.051	0.201	0.146	0.038	0.044	0.041	0.016	0.035	0.010	0.029
Ca	1.714	1.717	1.484	1.778	1.738	1.822	1.807	1.893	1.822	1.697	1.830
Na	0.534	0.595	0.345	0.088	0.828	0.692	0.712	0.787	0.827	0.872	0.907
K	0.129	0.133	0.185	0.062	0.124	0.261	0.250	0.183	0.211	0.177	0.197
A-site	0.377	0.470	0.014	0.001	0.709	0.797	0.790	0.871	0.878	0.751	0.948

Abbrevations: INT = intergrown with clinopyroxene, PH = phenocryst, GR = interstitial, RPX = rim on clinopyroxene, C = core, R = rim.

$$R \ln K^{\text{ol-cpx}}_{\text{Mg-Fe}^{2+}} = \frac{-1054}{T} + 0.23$$

where $K^{\text{ol-cpx}}_{\text{Mg-Fe}^{2+}} = (X^{\text{Mg}}/X^{\text{Fe}})_{\text{ol}}/(X^{\text{Mg}}/X^{\text{Fe}^{2+}})_{\text{cpx}}$ and R is the gas constant.

In the temperature interval 1300–1100°C $K^{\text{ol-cpx}}_{\text{Mg-Fe}^{2+}}$ ~0.80–0.75 according to the above equation. K_{D} values for the rocks of this study range from 0.85 to 0.20. Olivine compositions thus appear in many rocks to have been modified during cooling or as a result of alteration processes.

Pyroxenes

Representative pyroxene compositions are presented in Table 1. In clinopyroxene Mg-values (Mg/(Mg+ Fe^{2+})) range from 0.89 to 0.50. The highest ones are found in the clinopyroxenites from the Brandbukampen (BR), Ramvikholmen (RV) and Ravalsjøen (the small body northeast of Eiangen) (E) intrusions. The most magnesian clinopyroxenes also have the highest concentrations of Cr_2O_3, up to 0.74 wt. %. In the more iron-rich ones, Cr_2O_3 is negligible. Clinopyroxene is frequently zoned: Mg-value and Cr_2O_3 decrease from core to rim, MnO and Na_2O tend to increase. Al_2O_3 and TiO_2 are found both to increase (e.g. BR-2D) and decrease (e.g. BA-2) from core to rim. In the pyroxenites hour-glass and oscillatory zoning are common.

Ferric iron is calculated on the assumption that 4 cations are charge-balanced by 6 oxygens in the unit cell. Estimated Fe^{3+} contents vary considerably. Most samples have $Fe^{3+}/\Sigma Fe$ ratios of roughly 0.05, whereas ratios approaching and above 0.5 are found in some of the Brandbukampen (BR), Viksberget (VI), Dignes (DI) and Eiangen/Ravalsjøen (E) rocks (Table 1). It has recently been found that $^{\text{VI}}Fe^{3+}\text{-}^{\text{IV}}Al$ is one of the most important substitutional couples in terrestrial augites (Papike and White, 1979; Cameron and Papike, 1981; Basaltic Volcanism Study Project, 1981) and that the solubility of the $CaFe^{3+}AlSiO_6$ molecule in clinopyroxene is strongly favoured by high oxygen fugacity (Onuma, 1983). $Fe^{3+}/\Sigma Fe$ ratios similar to the highest ones estimated for pyroxenes in the Oslo rift gabbroic rocks are rarely reported, but have been observed among basaltic rocks in the Hocheifel area, West Germany, Hawaii and island arcs (Huckenholz, 1973; Basaltic Volcanism Study Project, 1981, Appendix A-12). The host rocks of

these pyroxenes thus appear to have crystallized under more oxidizing conditions than have most basaltic rocks.

With the exception of sample BA-2, where only a trace of orthopyroxene as reaction rim on olivine was found, orthopyroxene coexists with clinopyroxene relatively poor in Al_2O_3 (<4.0 wt. %).

Amphibole

The compositions of representative amphiboles are listed in Table 2. Dark brown amphibole occurring in rocks from the Brandbukampen (BR), Sønsteby-flakene (SØ-5 and SØ-6), Ballangrudkollen (BA) and Ravalsjøen (E) bodies is kaersutite with 4.0–7.3 wt. % TiO_2 and 10.4–16.0 wt. % Al_2O_3. Other rocks from Sønstebyflakene (SØ-1, 2, 3 and 4) contain common green hornblende with moderate contents of TiO_2 and Al_2O_3.

The stability relations of kaersutite in basaltic systems have been extensively studied by Helz (1973) at P_{H_2O} = 5 kbar. Although the Oslo Region gabbros are believed to have crystallized at considerably lower pressures, her findings appear pertinent to the origin of the kaersutite described here. Helz found a positive correlation between Ti (as Ti-tschermakite), Al^{IV} and temperature, and a marked decrease in the solubility of Ti with increasing oxygen fugacity. Kaersutite does not appear to be stable under conditions more oxidizing than those defined by the NNO-buffer or at temperatures below 950°C. The Mg/(Mg+Fe) ratio of hornblende is strongly dependent on that of the starting material, but also increases markedly with increasing oxygen fugacity.

The combination of Fe^{3+}-poor clinopyroxene and kaersutite found in some rocks suggests crystallization under relatively reducing conditions, such as those defined by the QFM buffer.

At Brandbukampen (BR) and Ravalsjøen (E-4, 5) kaersutite coexists with Fe^{3+}-rich clinopyroxene. This combination suggests crystallization in the more oxidizing part of the stability field of kaersutite, that is close to the NNO buffer. The observed decrease in TiO_2 and Al_2O_3 concentrations, and marked increase in Mg/(Mg+Fe) ratios from core to rim observed in BR-2D and BA-4, is compatible with a relative increase in oxygen fugacity during the final stages of crystallization. The presence of normal hornblende in the rocks SØ-1, 2, 3 and 4, suggests crystallization under more oxidizing conditions than those defined by the NNO buffer.

TABLE 3

Major element analyses and CIPW-norms in weight percent. Analyses marked IR from Ramberg (1970), and KF from Finstad (1972)

	SiO$_2$	TiO$_2$	Al$_2$O$_3$	Fe$_2$O$_3$	Feo	MnO	MgO	CaO	Na$_2$O	K$_2$O	P$_2$O$_5$	H$_2$O	Sum	Q	Qr	Ab
BR-1*	38.04	4.17	8.09	9.47	9.62	0.19	11.80	16.12	0.90	0.37	0.11	--	98.88	--	--	--
BR-2A*	42.45	3.75	12.37	6.09	9.26	0.19	9.00	13.93	1.68	0.97	0.21	--	99.90	--	5.73	5.32
BR-2B	39.05	3.96	14.26	6.48	7.47	0.15	9.43	12.89	2.41	1.55	1.46	--	99.11	--	9.16	1.69
BR-2D*	37.94	4.55	7.85	9.81	9.27	0.16	10.61	17.79	0.62	0.19	0.06	--	98.85	--	--	--
BR-KF	49.82	2.47	15.16	4.02	7.00	0.14	6.25	8.38	2.30	2.25	0.43	1.11	99.36	2.27	13.30	19.46
T-KF	48.61	2.31	14.78	3.86	6.21	0.23	6.94	7.89	4.23	2.64	0.61	1.62	99.95	--	15.60	24.34
S-1	46.19	2.90	14.88	6.00	8.80	0.22	6.68	10.55	2.64	1.06	0.37	--	100.29	--	6.26	22.34
S-KF	47.96	2.63	15.30	4.47	7.73	0.20	6.43	8.33	3.13	2.02	0.62	0.77	99.61	--	11.94	26.48
VI-1	49.22	2.48	17.39	4.26	7.61	0.18	4.64	8.58	3.55	2.01	0.40	--	100.32	--	11.88	30.04
VI-2	47.05	1.87	18.84	3.37	7.10	0.15	5.51	10.39	2.78	1.24	0.29	--	98.59	--	7.33	23.52
VI-3	46.15	2.81	15.61	4.53	10.20	0.20	6.26	8.84	3.00	1.62	0.36	--	99.58	--	9.57	23.90
VI-KF	45.51	3.12	17.05	4.05	7.05	0.32	6.30	10.19	2.87	1.05	1.04	1.42	99.98	--	6.20	24.28
BA-1	43.70	3.12	12.49	7.07	10.27	0.21	9.21	9.36	2.36	1.34	0.31	--	99.44	--	7.92	19.11
BA-2	47.21	2.33	12.13	4.13	9.62	0.19	10.07	10.08	2.44	1.32	0.31	--	99.83	--	7.80	20.65
BA-3	47.36	2.48	12.31	4.33	9.78	0.21	9.51	10.41	2.45	1.09	0.27	--	100.20	--	6.44	20.73
BA-4	44.16	3.13	16.27	6.95	8.20	0.19	4.87	11.16	2.57	1.06	0.30	--	98.88	--	6.26	18.91
BA-KF	44.97	2.73	11.73	4.00	8.39	0.22	10.33	10.09	2.44	1.32	0.45	2.06	98.78	--	7.80	18.66
HU-1*	45.64	2.30	6.30	5.36	9.50	0.20	12.90	14.01	1.40	0.74	0.19	--	98.54	--	4.37	11.43
HU-2	45.07	5.11	11.88	4.88	9.55	0.34	6.12	11.30	2.50	1.84	0.69	--	99.28	--	10.87	19.46
HU-4*	40.15	5.24	4.80	8.41	12.60	0.24	10.86	16.27	0.70	0.37	0.07	--	99.53	--	2.19	1.40
HU-5*	49.47	2.66	7.17	8.95	4.60	0.22	10.44	14.47	1.57	0.87	0.24	--	100.66	3.12	5.14	13.28
HU-7	43.53	4.00	8.98	7.07	12.36	0.21	8.92	10.87	2.01	0.94	0.00	--	98.90	--	5.48	17.01
HU-8*	45.42	3.45	7.20	5.69	10.50	0.20	10.53	14.64	1.31	0.61	0.16	--	99.71	--	3.60	11.08
HU-9	45.95	3.57	9.76	5.13	10.05	0.20	9.13	12.76	1.93	0.80	0.21	--	99.49	--	4.73	16.33
HU-KF	50.94	2.67	13.86	6.63	4.95	0.16	5.82	7.27	3.15	2.24	0.47	1.61	99.79	3.43	13.24	26.65
V-KF1*	48.86	1.15	2.81	4.14	7.25	0.20	17.45	15.93	0.45	0.04	0.06	1.12	99.66	--	0.24	3.81
V-IR2*	46.17	2.33	4.09	5.78	8.72	0.20	14.59	17.25	0.50	0.02	--	--	99.70	--	0.12	4.23
V-IR3	47.20	3.79	13.88	2.29	13.13	0.29	6.56	8.54	2.55	0.66	--	--	98.89	--	3.90	21.58
V-IR4*	37.86	5.31	4.40	12.00	12.05	0.40	11.33	15.13	0.47	0.10	--	--	99.05	--	--	--
V-IR5	49.94	3.03	16.01	4.31	7.97	0.39	3.56	5.48	4.26	3.45	--	--	98.40	--	20.39	30.37
AU-1*	45.30	1.00	3.74	4.69	7.54	0.17	21.53	13.79	0.39	0.13	0.04	--	98.32	--	0.77	3.30
AU-2*	45.85	1.14	4.15	4.02	7.33	0.15	19.50	14.97	0.44	0.14	0.04	--	97.73	--	0.83	3.72
AU-KF	45.65	2.41	10.93	3.80	10.03	0.21	10.13	9.86	2.34	1.10	0.43	2.42	99.35	--	6.50	19.80
AU-B1	47.30	2.27	15.94	5.70	6.39	0.25	3.94	7.12	4.85	5.52	1.32	--	98.60	--	14.89	28.76
DI-1	49.36	2.66	18.61	3.73	7.18	0.17	4.22	6.93	4.85	1.94	0.78	--	100.43	--	11.46	34.94
DI-2	49.36	2.40	18.85	2.90	8.26	0.18	3.36	6.56	5.10	2.21	1.32	--	100.50	--	13.65	34.81
DI-3	48.60	2.72	17.96	3.05	9.12	0.20	3.73	6.29	4.94	2.20	1.29	--	100.11	--	13.00	34.76
DI-4A	50.77	2.58	18.89	2.95	7.00	0.18	3.64	7.18	4.85	1.99	0.83	--	100.86	--	11.76	37.52
DI-4B	50.96	2.63	18.61	3.19	7.04	0.18	3.43	7.08	4.85	2.04	0.86	--	100.87	--	12.06	38.67
DI-7	49.80	2.95	18.31	3.35	7.90	0.18	3.96	6.92	4.85	1.99	0.84	--	101.05	--	11.76	35.87
SØ-1	52.53	2.42	15.18	4.03	7.65	0.15	4.57	7.33	3.26	1.56	0.49	--	99.17	5.65	9.22	27.58
SØ-2	50.11	2.55	14.72	5.62	7.47	0.16	5.62	8.90	2.85	1.24	0.32	--	99.56	3.85	7.33	24.12
SØ-3	53.60	2.63	14.53	5.42	6.32	0.15	4.83	7.33	3.25	1.81	0.37	--	100.24	7.59	10.70	27.50
SØ-4*	43.95	1.23	24.59	4.07	4.67	0.17	5.37	12.21	1.80	0.25	0.10	--	98.41	--	1.48	15.23
SØ-5	48.91	2.12	17.37	3.92	5.68	0.12	4.51	8.50	4.80	1.01	1.26	--	98.20	--	5.97	38.96
SN-1	50.97	2.53	15.17	8.71	5.75	0.21	3.01	6.92	3.81	1.81	1.23	--	100.12	6.08	10.70	32.24
SN-2	55.14	1.70	16.03	4.87	6.89	0.19	2.59	5.78	3.14	0.80	--	--	101.09	4.75	18.56	33.51
SN-5	49.49	3.31	12.05	8.70	9.40	0.25	3.29	6.09	2.70	3.09	1.35	--	99.72	7.61	18.26	22.85
SN-7	52.44	2.78	13.17	7.29	7.54	0.26	3.42	6.59	3.55	2.44	1.00	--	100.48	7.25	14.42	30.04
E-1*	45.24	1.16	12.15	3.52	10.60	0.20	17.29	6.97	1.95	0.61	0.18	--	99.87	--	3.60	16.50
E-2	52.33	1.36	16.68	3.41	5.90	0.20	7.51	7.58	3.73	1.48	0.44	--	100.62	--	8.75	31.56
E-3*	45.85	1.05	13.03	2.55	10.21	0.18	16.74	7.42	2.04	0.73	0.13	--	99.93	--	4.31	17.26
E-4*	45.05	2.59	8.68	4.48	7.76	0.17	12.76	14.07	1.72	1.21	0.28	--	98.77	--	7.15	5.45
E-5*	44.53	2.31	8.23	4.51	7.54	0.18	14.46	13.19	1.48	1.62	0.25	--	98.30	--	9.57	2.00

Sample abbreviations: BR = Brandbukampen; T = Tingelstad; S = Sølvsberget; VI = Viksberget; BA = Ballangrudkollen; HU = Husebykollen; RV = Ramvikholmen; V = Vestby; AU = Aurenhaugen; DI = Dignes; SØ = Sønstebyflakene; SN = Snaukollen; E = Eiangen/Ravalsjøen.
* = cumulates.

	An	Ne	Lc	Di	Hd	En	Fs	Fo	Fa	Ml	Il	Mt	Ap
BR-1*	16.94	4.43	1.71	22.58	8.53	–	–	26.52	12.66	8.63	7.92	8.22	0.26
BR-2A*	23.35	4.82	–	27.01	8.64	–	–	6.93	2.80	–	7.12	7.61	0.50
BR-2B	23.51	10.13	–	22.51	1.76	–	–	9.14	0.90	–	7.52	9.40	3.44
BR-2D*	18.08	2.84	0.88	40.53	2.28	–	–	10.70	0.76	5.52	8.64	14.22	0.14
BR-KF	24.40	–	–	8.74	2.80	11.51	4.23	–	–	–	4.69	5.83	1.01
T-KF	13.54	6.20	–	13.87	3.38	–	–	7.60	2.34	–	4.39	5.60	1.44
S-1	25.62	–	–	14.42	5.15	3.33	1.36	4.64	2.10	–	5.51	8.70	0.87
S-KF	21.73	–	–	9.23	3.28	3.37	1.38	5.86	2.63	–	5.00	6.48	1.46
VI-1	25.58	–	–	7.77	3.92	0.44	0.26	5.26	3.36	–	4.71	6.18	0.94
VI-2	35.27	–	–	7.93	3.75	1.04	0.56	6.31	3.77	–	3.55	4.89	0.68
VI-3	24.34	0.80	–	8.77	5.26	–	–	8.08	6.12	–	5.34	6.57	0.85
VI-KF	30.54	–	–	8.27	2.32	3.98	1.28	5.52	1.96	–	5.93	5.87	2.45
BA-1	19.53	0.47	–	15.20	4.77	–	–	11.14	4.42	–	5.93	10.25	0.73
BA-2	18.25	–	–	17.45	6.53	1.25	0.54	11.03	5.21	–	4.43	5.99	0.73
BA-3	19.37	–	–	17.33	7.36	2.37	1.15	9.31	5.00	–	4.71	5.77	0.64
BA-4	29.73	1.54	–	11.21	8.27	–	–	4.86	4.53	–	5.94	6.71	0.71
BA-KF	17.16	1.08	–	18.86	5.11	–	–	11.90	4.08	–	5.19	5.80	1.06
HU-1*	8.72	0.22	–	37.77	9.83	–	–	10.24	3.37	–	4.37	7.77	0.45
HU-2	15.76	0.92	–	21.69	7.07	–	–	3.64	1.50	–	9.71	7.08	1.63
HU-4*	8.86	2.45	–	45.24	11.84	–	–	3.94	1.30	–	9.95	12.19	0.17
HU-5*	9.95	–	–	44.04	3.30	5.59	0.48	–	–	–	5.05	10.17	0.57
HU-7	14.74	–	–	22.35	9.33	6.73	3.23	3.59	1.89	–	7.60	0.25	0.00
HU-8*	11.96	–	–	36.58	11.26	2.71	0.96	4.59	1.79	–	6.55	8.25	0.38
HU-9	15.61	–	–	27.93	9.31	2.93	1.12	4.81	2.03	–	6.78	7.44	0.50
HU-KF	17.06	–	–	10.97	1.64	9.41	1.62	–	–	–	5.07	7.99	1.11
V-KF1*	5.53	–	–	49.64	8.33	14.89	2.87	3.90	0.83	–	2.18	6.00	0.14
V-IR2*	8.86	–	–	47.25	14.29	2.01	0.70	8.70	3.33	–	4.43	5.55	–
V-IR3	24.48	–	–	7.87	6.93	9.12	9.21	2.50	2.78	–	7.20	3.32	–
V-IR4*	9.60	2.15	0.46	31.63	16.68	–	–	19.00	12.67	2.22	10.09	9.87	–
V-IR5	14.37	3.08	–	6.30	4.21	–	–	4.17	3.52	–	5.75	6.25	–
AU-1*	8.07	–	–	38.99	8.91	0.94	0.25	24.25	7.01	–	1.90	3.62	0.09
AU-2*	8.94	–	–	42.66	9.15	1.58	0.39	19.07	5.17	–	2.17	3.83	0.09
AU-KF	16.07	–	–	17.29	6.98	2.34	1.08	10.43	5.32	–	4.58	5.51	1.01
AU-B1	14.28	6.65	–	5.82	4.41	–	–	4.99	4.78	–	4.31	5.47	3.11
DI-1	23.28	3.30	–	3.25	1.63	–	–	6.31	3.99	–	5.05	5.41	1.84
DI-2	21.72	4.52	–	0.94	0.89	–	–	5.56	6.70	–	4.56	4.20	3.11
DI-3	20.33	3.86	–	1.06	1.01	–	–	6.17	7.39	–	5.17	4.42	3.04
DI-4A	23.90	1.90	–	3.18	1.98	–	–	5.32	4.20	–	4.90	4.28	1.96
DI-4B	22.98	1.26	–	3.25	2.09	–	–	4.93	4.00	–	5.00	4.63	2.03
DI-7	22.31	2.80	–	3.27	2.08	–	–	5.85	4.71	–	5.60	4.86	1.98
SØ-1	22.18	–	–	5.82	3.12	8.68	5.34	–	–	–	4.60	5.84	1.16
SØ-2	23.71	–	–	11.16	3.59	8.83	3.25	–	–	–	4.84	8.15	0.17
SØ-3	19.71	–	–	9.28	2.06	7.73	1.97	–	–	–	5.00	7.86	0.87
SØ-4*	58.28	–	–	1.07	0.24	5.63	1.47	5.08	1.46	–	2.34	5.90	0.24
SØ-5	22.87	0.70	–	6.81	2.07	–	–	5.66	2.17	–	4.03	5.68	2.97
SN-1	18.95	–	–	4.26	1.68	5.52	2.49	–	–	–	4.81	10.75	2.90
SN-2	16.69	–	–	3.04	2.54	5.04	4.82	–	–	–	3.23	7.06	1.89
SN-5	11.63	–	–	5.16	2.79	5.80	3.59	–	–	–	6.29	12.61	3.18
SN-7	12.79	–	–	7.81	2.97	4.90	2.14	–	–	–	5.28	10.57	2.36
E-1*	22.60	–	–	6.65	2.02	5.82	1.84	24.32	9.34	–	2.20	5.10	0.42
E-2	24.40	–	–	6.43	1.84	10.93	3.59	3.36	1.22	–	2.58	4.94	1.04
E-3*	24.24	–	–	7.14	2.28	2.55	0.93	25.11	10.12	–	1.99	3.70	0.31
E-4*	12.39	4.67	–	37.37	6.75	–	–	10.13	2.31	–	4.92	6.50	0.66
E-5*	11.03	5.23	–	36.03	5.79	–	–	13.53	2.75	–	4.39	6.54	0.59

TABLE 4

Trace element concentrations and $^{87}Sr/^{86}Sr$ ratios in gabbroic Oslo rift rocks (abbreviations as in Table 3)

Sample	Sc	Cr	Co	Ni	Rb	Sr	Cs	Ba	La	Ce	Nd	Sm	Eu
BR-1*	60	30	81.2	24	5.5	288	0.31	185	14.1	33	–	5.07	1.6
BR-2A*	43	177	63.8	94	18.6	709	0.22	362	23.6	50	–	5.97	2.1
BR-2B	42	54	55.8	88	33.7	928	0.85	646	49.7	104	–	12.2	3.5
BR-2D*	85	136	82.8	194	3.4	188	0.10	51	10.9	29	–	5.19	1.5
BR-KF	–	–	–	–	–	–	–	–	31.2	76	38.7	7.06	1.8
T-KF	–	–	–	–	–	–	–	–	64.8	123	58.5	9.93	2.1
S-1	37	52	55.2	83	28.6	706	0.52	261	32.2	58	–	7.83	2.5
S-KF	–	–	–	–	–	–	–	–	41.3	94	40.0	7.60	1.8
VI-1	20.0	32	34.6	<10	52.7	917	0.37	570	51.3	83	–	8.07	2.2
VI-2	21.7	91	42.6	<10	31.5	898	0.70	354	31.5	64	–	5.74	1.6
VI-3	26.2	56	57.4	<10	43.5	797	0.75	395	48.1	71	–	7.01	2.1
VI-KF	–	–	–	–	–	–	–	–	44.7	80	45.4	11.0	2.2
BA-1	42	n	72.2	128	36.4	672	0.84	525	33.8	64	–	6.30	2.0
BA-2	46	n	62.0	116	36.7	639	2.34	426	37.8	74	–	6.89	2.1
BA-3	37	n	62.4	121	25.9	605	0.62	483	30.7	59	–	6.55	2.0
BA-4	33	n	49.3	46	27.5	1010	1.10	469	32.2	59	–	5.92	1.9
BA-KF	–	–	–	–	–	–	–	–	34.9	80	41.4	7.52	2.0
HU-1*	50	41	77.4	126	14.9	424	1.34	400	39.8	66	–	7.20	2.1
HU-2	45	7	40.0	<10	95.7	1000	3.20	567	56.5	111	–	12.4	3.7
HU-3	–	–	–	–	–	–	–	–	–	–	–	–	–
HU-4*	81	–	89.5	96	15.9	177	1.00	413	13.1	29	–	4.56	1.3
HU-5*	72	–	54.2	94	23.8	353	0.77	97	27.4	58	–	8.59	2.5
HU-7	53	–	82.1	98	29.3	532	2.22	566	30.8	72	–	7.72	2.2
HU-8*	52	–	79.6	176	22.4	498	1.87	n	19.2	58	–	6.54	1.9
HU-9	54	–	72.4	106	36.9	787	1.94	151	27.9	52	–	6.74	2.3
HU-KF	–	–	–	–	–	–	–	–	42.9	94	42.2	8.78	2.0
V-KF*	–	–	–	–	–	–	–	–	6.4	18	11.9	3.58	1.1
V-EI2*	75	275	91.5	73	–	–	0.27	15	5.3	12	–	2.10	0.68
V-I6*	94	428	88.1	153	n	n	0.05	12	12.2	23	–	3.34	1.21
AU-1*	60	21	98.4	393	3.3	68	0.35	58	5.1	18	–	3.31	0.69
AU-2*	74	1072	88.8	404	3.3	93	0.43	110	6.4	22	–	2.78	0.91
AU-KF	–	–	–	–	–	–	–	–	30.2	61	30.5	5.38	1.55
AU-B1	8.9	<2	23.4	11	105	1623	4.23	1027	150	218	–	18.7	4.86
DI-1	11.5	42	30.3	42	48.1	1053	0.78	535	66.0	124	–	15.2	4.07
DI-2	8.1	17	27.3	22	60.5	1148	0.70	660	92.6	180	–	19.8	5.27
DI-3	8.6	45	30.9	<10	60.6	1108	1.05	602	82.5	150	–	15.5	5.05
DI-4A	12.3	11	23.0	48	50.0	1075	1.24	384	60.7	137	–	13.5	3.83
DI-4B	12.8	36	23.0	20	53.0	1046	1.55	462	65.9	147	–	13.5	4.04
DI-7	12.1	39	30.2	35	49.7	1038	0.76	445	59.4	122	–	13.3	3.59
SØ-1	24.3	49	25.1	12	73.5	413	3.86	208	40.8	95	–	9.26	2.45
SØ-2	30	50	13.6	63	36.2	433	2.12	279	27.3	75	–	6.82	1.65
SØ-3	25.5	16	15.3	<10	53.8	420	1.49	349	31.9	78	–	7.41	1.89
SØ-4*	6.1	153	4.9	63	5.0	819	1.75	82	7.4	16	–	1.40	0.59
SØ-5	19.7	10	31.9	21	38.3	655	1.44	239	49.7	131	–	13.9	3.86
SN-1	17.4	41	29.7	–	59.3	507	1.39	306	62.7	124	–	18.8	5.38
SN-2	12.2	42	17.5	–	103	468	1.99	505	75.7	138	–	19.6	5.59
SN-5	19.9	8	35.4	27	119	338	3.60	514	78.0	168	–	21.7	5.45
SN-7	21.7	36	27.9	117	80.5	423	0.51	303	61.2	124	–	19.2	5.14
E-1*	17.2	28	94.4	544	16.5	468	0.23	219	20.5	37	–	3.79	1.11
E-2	16.8	36	33.2	111	51.3	564	1.53	448	72.9	127	–	10.2	1.57
E-3*	17.4	25	96.1	422	21.2	479	0.32	207	19.9	37	–	3.12	1.09
E-4*	39	687	67.8	224	39.5	632	1.13	443	43.2	91	–	7.01	1.81
E-5*	39	767	70.1	316	43.8	375	2.77	432	44.8	74	–	6.76	1.95

* = cumulates.

TABLE 4 (continued)

Sample	Gd	Tb	Yb	Lu	Hf	Ta	Th	U	$^{87}Sr/^{86}Sr$
BR-1*	—	0.56	1.5	0.26	3.70	1.02	0.66	0.22	0.70395
BR-2A*	—	0.83	2.8	0.40	3.40	2.05	2.2	0.58	0.70402
BR-2B	—	1.6	3.2	0.47	4.53	2.71	3.4	1.0	—
BR-2D*	—	0.88	3.4	0.55	4.10	0.72	0.46	0.12	—
BR-KF	6.3	0.95	2.4	0.34	—	—	—	—	—
T-KF	7.5	0.84	1.8	0.26	—	—	—	—	—
S-1	—	0.87	2.9	0.37	3.59	1.90	2.6	0.69	0.70490
S-KF	6.8	0.83	2.1	0.33	—	—	—	—	—
VI-1	—	0.78	1.8	0.30	7.54	3.52	5.4	1.3	0.70525
VI-2	—	0.83	1.7	0.34	5.03	2.50	3.3	0.87	0.70454
VI-3	—	1.04	2.0	0.28	7.65	3.46	4.4	1.1	—
VI-KF	8.7	1.27	4.1	0.69	—	—	—	—	—
BA-1	—	1.00	2.6	0.45	4.27	3.15	4.5	n	0.70513
BA-2	—	1.06	2.8	0.45	4.38	2.33	3.8	n	0.70467
BA-3	—	1.02	2.7	0.47	3.85	2.11	2.5	n	0.70520
BA-4	—	0.94	2.8	0.52	3.50	2.02	3.2	n	0.70465
BA-KF	7.2	1.12	2.8	0.40	—	—	—	—	—
HU-1*	—	0.78	2.1	0.33	3.08	1.56	1.1	0.28	0.70457
HU-2	—	1.59	2.4	0.34	7.32	4.52	6.6	2.3	0.70707
HU-3	—	—	—	—	—	—	—	—	0.71187
HU-4*	—	0.70	1.4	0.22	3.34	1.22	1.0	—	—
HU-5*	—	1.44	2.7	0.36	4.03	1.80	2.2	0.51	—
HU-7	—	1.28	2.4	0.38	5.64	2.07	2.8	0.75	—
HU-8*	—	0.82	2.2	0.35	3.41	1.23	1.5	—	—
HU-9	—	0.85	3.7	0.61	4.18	2.39	2.5	—	—
HU-KF	6.8	0.86	1.6	0.20	—	—	—	—	—
V-KF*	3.8	0.40	1.1	0.18	—	—	—	—	—
V-EI 2*	—	0.21	<0.5	0.08	1.51	0.44	n	n	—
V-I 6*	—	0.29	0.70	0.06	2.22	0.25	n	n	—
AU-1*	—	0.50	1.2	0.15	1.66	0.23	0.31	0.09	0.70492
AU-2*	—	0.43	1.2	0.18	1.51	0.37	0.30	0.09	0.70450
AU-KF	5.73	0.73	1.5	0.23	—	—	—	—	—
AU-B1	—	2.09	4.4	0.81	13.1	10.4	15.0	4.5	0.70518
DI-1	—	2.44	4.3	0.52	10.0	5.09	7.1	—	0.70505
DI-2	—	2.44	5.0	0.68	12.6	6.52	8.8	—	0.70442
DI-3	—	2.14	3.1	0.30	19.0	6.91	8.4	2.6	0.70451
DI-4A	—	1.86	3.2	0.56	13.6	5.72	7.0	2.1	0.70463
DI-4B	—	1.88	3.4	0.63	15.9	6.13	8.1	2.4	—
DI-7	—	2.05	3.4	0.69	13.3	5.74	6.5	2.1	—
SØ-1	—	1.44	4.8	0.81	6.2	1.89	5.5	1.7	0.70848
SØ-2	—	0.98	2.3	0.36	6.1	1.69	3.4	0.8	0.70685
SØ-3	—	1.13	3.3	0.48	7.1	1.87	4.9	1.5	0.70724
SØ-4*	—	0.13	0.22	0.04	1.18	0.50	0.63	0.18	0.70436
SØ-5	—	2.06	3.7	0.50	9.0	2.67	3.9	1.2	0.70511
SN-1	—	2.60	5.6	0.97	10.5	4.33	7.5	2.3	0.70515
SN-2	—	2.42	6.6	0.90	14.8	4.77	9.9	3.0	0.70634
SN-5	—	2.89	6.8	0.98	15.9	5.73	8.5	2.5	0.70773
SN-7	—	2.71	5.5	0.77	12.6	4.92	8.1	2.5	0.70607
E-1*	—	0.62	2.7	0.34	2.32	1.16	1.5	1.0	0.70514
E-2	—	1.34	3.4	0.48	9.9	6.00	8.8	3.0	—
E-3*	—	0.54	1.5	0.22	5.08	1.47	2.4	0.92	—
E-4*	—	0.69	0.88	0.15	5.76	3.58	2.2	0.78	0.70540
E-5*	—	0.69	0.81	0.12	6.7	3.74	3.6	1.1	0.70632

Plagioclase

Plagioclase phenocrysts are generally strongly zoned with calcic cores and more sodic rims. The most calcic cores (An_{83}–An_{80}) are found in samples from Sølvsberget (S), Viksberget (VI), Ballangrudkollen (BA) and Snaukollen (SN). Even groundmass plagioclase in Brandbukampen has An contents up to 81 mol.%. The orthoclase content is less than 2 mol.% in the most calcic plagioclase, but increases slightly with increasing Na concentration. K-rich alkali feldspar occurs in the groundmass in some rocks.

Plagioclase in the Dignes (DI) and Sønstebyflakene (SØ) rocks has less calcic cores ($An_{50}Ab_{48}Or_2$) and more potassic rims ($An_{16}Ab_{71}Or_{13}$) than those described above. This trend is similar to that of feldspars in the intrusive larvikites (Neumann, 1980) and extrusive rhomb porphyries (Harnik, 1969; Larsen, 1978).

Whole rock compositions

Whole rock analyses (Table 3) were done by flame photometry (Na), atomic absorption (Mg), and X-ray fluorescence (XRF) analysis of fused pellets (other major elements). Fe^{2+} was determined by titration. Rb and Sr were analyzed by XRF on pressed pellets, other trace elements (Table 4) by instrumental activation analysis methods described by Gordon et al. (1968) and Brunfelt and Steinnes (1969). Norms are given in cation percentages. Tables 3 and 4 include analyses by Ramberg (1970) (major elements) and Finstad (1972) (major elements, and rare earth elements (REE) by radiochemical neutron activation analysis).

Strontium isotopic determinations were made by solid source mass-spectrometry using the method described in Jacobsen and Heier (1978). The $^{87}Sr/^{86}Sr$ ratios measured were corrected for age using the Rb and Sr concentrations from the trace element analyses for $^{87}Rb/^{86}Sr$ calculations, and an average age of 266 million years to obtain the inital $^{87}Sr/^{86}Sr$ ratios.

Rocks with clinopyroxene phenocrysts vary considerably in composition. Samples with moderate proportions of phenocrysts (BR-2A, 2B, KF; HU-2, 7, 9; and E-4, 5) have 5–11 wt. % MgO, Th-concentrations between 2.5 and 4.5 ppm, and strongly light-REE-enriched chondrite-normalized REE-patterns

(La/Lu: 100–367) (Fig. 2). Pyroxene-rich rocks with cumulate textures (BR-1, 2D; HU-4, 5, 8; V-KF1, IR2, IR4; 16; E12; AU-1, 2; and E-4, 5) are very rich in MgO (10.5–21.5 wt. %) and CaO (13.8–17.8 wt. %). Ratios Mg/Fe^{2+} are similar in rocks and clinopyroxene phenocrysts. Concentrations of Al_2O_3, alkalies and incompatible trace elements are low, and REE patterns relatively flat (Fig. 2). Concentrations of Cr and Sc (elements which are preferentially partitioned into Ca-rich pyroxene) tend to be high. The chemical data thus support the textural evidence that these rocks are cumulates. This is well demonstrated among the Brandbukampen (BR) rocks. The compositional change from BR-2B (e.g., 24% norm. cpx, 50 ppm La, La/Lu = 106) through BR-2A (36% norm. cpx, 24 ppm La, La/Lu = 59) to BR-2D (43% norm. cpx, 11 ppm La, La/Lu = 20) (Tables 3, 4, Fig. 2) is compatible with the assumption that BR-2A and BR-2D consist of clinopyroxene and Fe-Ti oxides (in the ratio 80:20) with about 50 and 20% respectively of trapped liquid of BR-2B composition.

The plagioclase-rich rocks from Sølvsberget (S), Viksberget (VI), Dignes (DI), Sønstebyflakene (SØ), Snaukollen (SN), and Eiangen (E-2) have 2.6–7.5 wt. % MgO, high concentrations of incompatible elements, and strongly light-REE-enriched REE patterns (La/Lu = 62–185) (Fig. 2). Weak negative Eu anomalies are common. Sample SØ-4, however, has the positive Eu-anomaly, relatively high Sr and low incompatible element concentrations (Tables 3, 4, Fig. 2) (e.g. Sr/Th = 1300) typical of plagioclase cumulates. However, sample SØ-4 has a less pronounced positive Eu-anomaly than a hypothetical cumulate plotted for comparison in Fig. 2, assuming T-f_{O_2} conditions representative of the QFM buffer (Drake and Weill, 1975). The REE data thus support the conclusion presented above that the rocks SØ-1, 2, 3, 4 crystallized under more oxidizing conditions than those defined by the NNO buffer.

Also the Dignes (DI) rocks and the Aurenhøgda sample AU-B1 are very rich in Sr (1038–1623 ppm) (Table 4). Such high concentrations of Sr in rocks with plagioclase phenocrysts are easily interpreted as the result of accumulation of plagioclase. However, these rocks have some of the lowest CaO concentrations found in this study (Table 3), are highly enriched in incompatible elements (e.g., 6.5–15.0 ppm Th), and have weak negative Eu anomalies. Sr/Th ratios are 110–150, which place them in the lower part of the range covered by aphyric basaltic
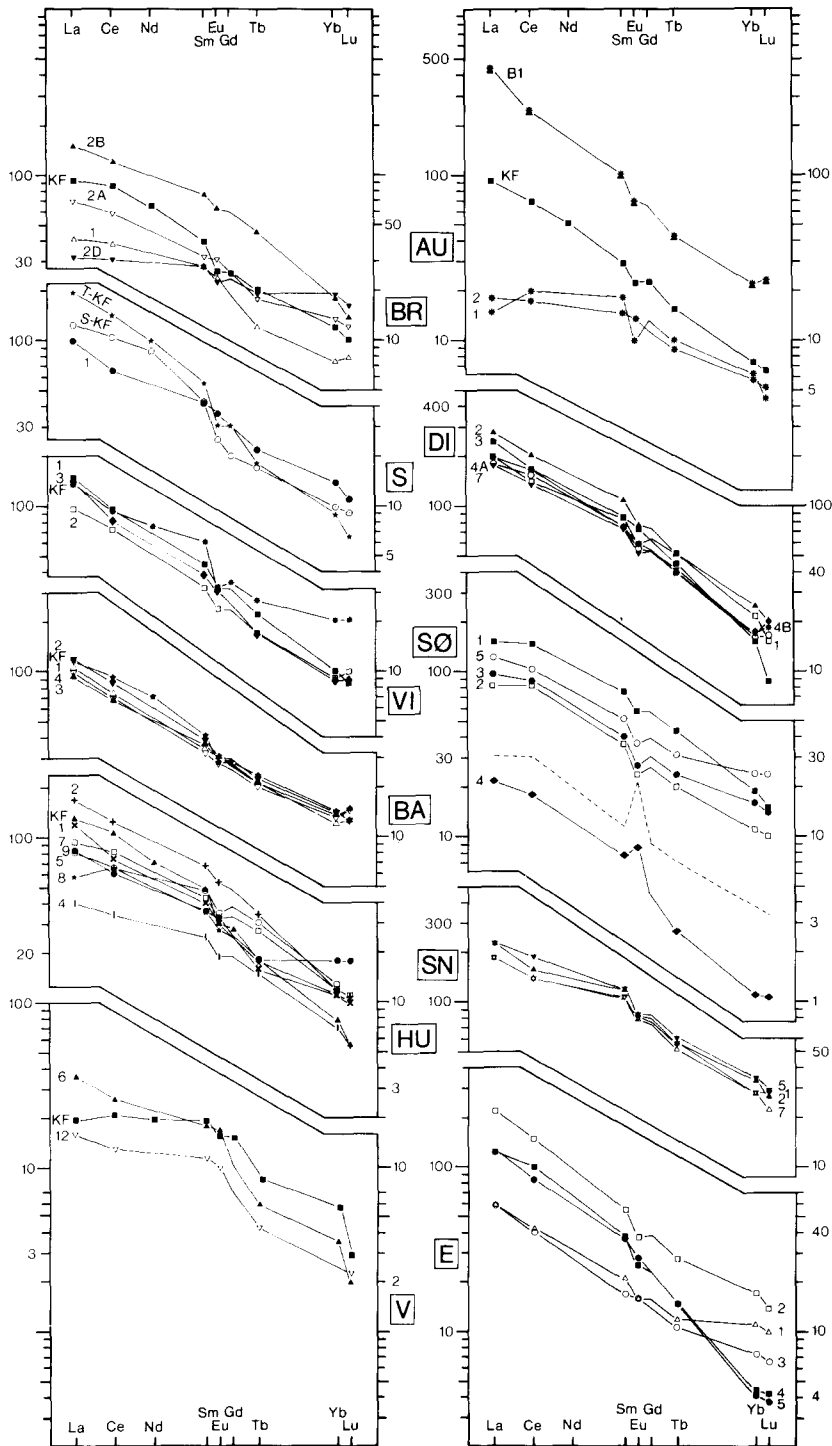
Fig. 2. Chrondrite-normalized REE patterns of rocks from the Oslo rift gabbroic intrusions. For comparison the REE pattern of a hypothetical cumulate consisting of 70% plagioclase plus 30% melt of the type SØ-2 (open squares) is indicated as a dashed line. Partition coefficients plagioclase/melt used in the estimate are those given by Drake and Weill (1975) for T-f_{O_2} conditions corresponding to the QFM buffer. Abbreviations as in Fig. 1. Sample numbers are given.

lavas of similar composition in the Oslo rift (120–500) (Weigand, 1975; O. Steinlein and E.-R. Neumann, unpublished data). Concentrations of Cr, Co and Ni are low. It is therefore concluded that the Dignes (DI) rocks and sample AU-B1 are not cumulates, but represent melt compositions.

The olivine-rich samples E-1 and E-3 have chemical indications of cumulate olivine (high contents of MgO, Co and Ni, low ones of incompatible elements) (Tables 3, 4).

Rocks which are believed to contain cumulate minerals are marked with an asterisk in Tables 3 and 4. Other rocks are believed to represent melt compositions.

Rb-Sr isotope data

Rb and Sr isotope compositions were determined on 31 selected whole rock samples, plus mineral separates of sample DI-6. The results are plotted in Fig. 3.

The Snaukollen whole rock samples and separated clinopyroxene, plagioclase, apatite and biotite from the Dignes sample DI-6 define isochrons of similar age (265 ± 11 and 266 ± 5 Ma) and with initial $^{87}Sr/^{86}Sr$ ratios of 0.70380 ± 5 and 0.70394 ± 15 respectively (Fig. 3B).

Whole rock samples from the other intrusions of this study do not define isochrons. The highest $^{87}Sr/$
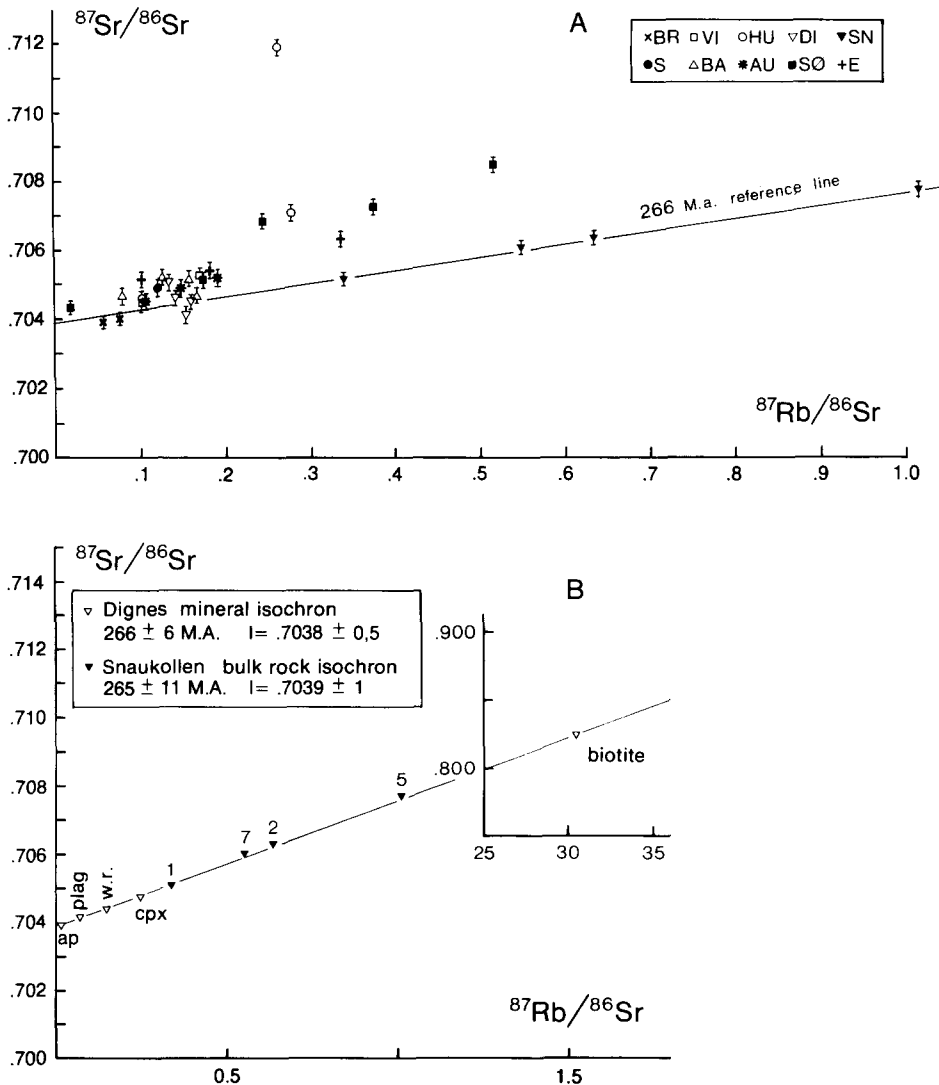
Fig. 3. Rb-Sr isotope data for Oslo rift gabbroic rocks. Symbols as in Fig. 3 with 2σ error bars. A. Bulk rock data for all samples analyzed. The 266 Ma isochron from Fig. 3B is included for comparison. B. Bulk rock isochron defined by the Snaukollen samples and mineral isochron defined by the Dignes DI-6 minerals.

[86]Sr ratios relative to the 266 Ma isochron are found in the Husebykollen samples HU-2 and HU-4 and the Sønstebyflakene rocks SØ-1, 2 and 3. The dispersion of data in Fig. 3A may reflect contamination or mixing between magmas with different isotopic signatures. This possibility is tested in Fig. 4 which shows initial $^{87}Sr/^{86}Sr$ ratios plotted against Sr. Faure (1977) has shown that magma mixing (or contamination) products will define a hyperbola in such a diagram. Both the Dignes and the Sønstebyflakene datapoints fall close enough to hypothetical mixing

trends (A-B and C-D in Fig. 4) to suggest that their Sr isotope ratios are affected by mixing or contamination processes.

Discussion

Classification

The mafic intrusions in the Oslo rift range from gabbros, clinopyroxenites, and anorthosites to dioritic and monzonitic rocks. Both textural and chemical
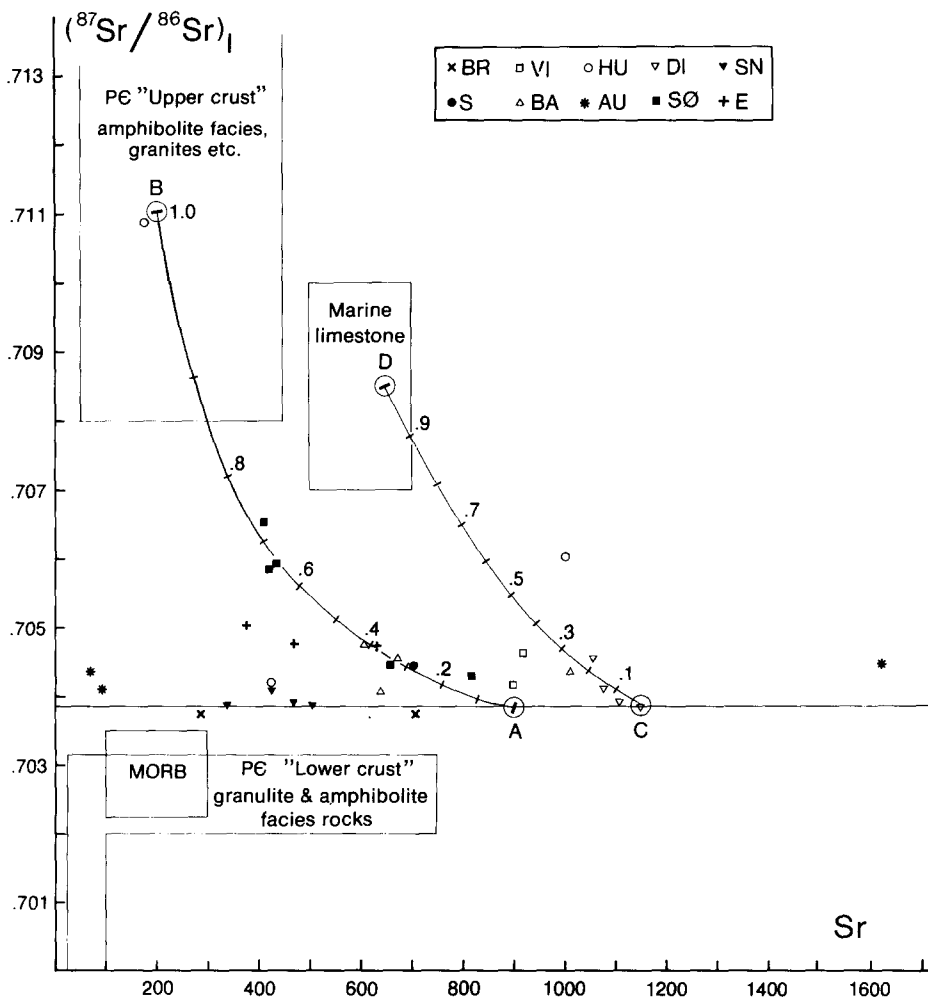
Fig. 4. Initial $^{87}Sr/^{86}Sr$ ratios plotted against Sr for Oslo rift gabbroic rocks. Compositional ranges found among mid-ocean ridge basalts (MORB) (Basaltic Volcanism Study Project, 1981), marine limestones (Faure, 1977) and Precambrian rocks in southeast Norway (Jacobsen and Heier, 1978; B. Sundvoll, unpublished data) are indicated by boxes. The trends A-B and C-D represent mixing between hypothetical, somewhat evolved, mantle-derived magmas (A and C) and possible upper crustal contaminants (B: Precambrian amphibolite facies rocks, granites, etc.; D: Cambro-Silurian carbonaceous sedimentary rocks). Numbers indicate fractions of contaminant in the mixture. The Sønstebyflakene (SØ) samples fall close to the A-B, the Dignes (DI) rocks close to the C-D mixing trend. Symbols as in Fig. 3.

data indicate that some of the rocks are cumulates.

The olivine tholeiitic character of most of the rocks is verified by the fact that a number of them carry modal ol + opx (Table 1), and that normative mineral assemblages of most rocks put them within, or close to, the olivine tholeiitic portion of the basalt tetrahedron (Table 3). The terms "essexite" or "Oslo-essexite", are therefore not appropriate, and we suggest that for general purposes they simply be called "gabbros" or "gabbroic rocks".

Position of the gabbroic rocks in the rift history

The Rb-Sr Snaukollen whole rock and Dignes mineral isochrons of 265 ± 11 and 266 ± 5 Ma, respectively, imply emplacement of the mafic intrusions at a relatively late stage of the rifting period (304–245 Ma ago). Compositionally the gabbroic rocks resemble the younger basalts, those at B_2 and B_3 stratigraphic positions, which are also silica-saturated to mildly undersaturated, strongly enriched in incompatible elements and in light relative to heavy REE. These data thus support the view that the mafic intrusions may represent feeders to late stage central volcanoes.

Source materials

The mafic silicates in the Oslo rift gabbroic rocks have the following range in Mg-values: 0.79–0.39 in olivine, 0.86–0.34 in clinopyroxene, and 0.76–0.53 in orthopyroxene (Table 1). A considerable compositional range is found within each intrusive body.

Primary mantle-derived basaltic magmas are expected to be in equilibrium with olivines ranging from Fo_{95} to Fo_{88}, and have Mg-values between 0.86 and 0.69 (e.g., Mysen and Kushiro, 1977; Hanson and Langmuir, 1978; Basaltic Volcanism Study Project, 1981). Even the most magnesian olivines of this study are thus less magnesian than those expected to be in equilibrium with primitive basaltic melts. The olivines appear to have suffered subsolidus reequilibration. Conclusions concerning melt compositions can thus not be based on olivines. Estimates of Mg-Fe relations in those melts which gave rise to the most mafic rocks of the present study are therefore based on clinopyroxene compositions.

The clinopyroxene-liquid relations described by the formula

$$\ln K^{cpx-L}_{Mg-Fe^{2+}} = \frac{1651}{T} + 0.3133$$

(Nielsen and Drake, 1979), imply that at a temperature of roughly 1200°C, the most magnesian clinopyroxene (Mg-value = 0.89 in RV-11, E-5; Table 1) crystallized from melts with a Mg-value of 0.66, significantly different from the range covered by primitive magmas. None of the rocks thus appear to have formed from primitive melts, but from melts which have been subjected to some degree of fractional crystallization or contamination.

Fractional crystallization

It has been concluded above that no rock of the present study has formed from a primitive mafic magma. The complexity of the evolutionary history of these rocks is reflected in the variety of crystallization orders (a–f) listed above, in the range of mineral compositions and in their chemical diversity.

The observed differences in crystallization order (which occur both between and within plugs) are such that they would not be expected to represent different stages of crystallization from identical initial melts under similar physical conditions. Instead, they would seem to reflect either compositional differences inherited from the parental magma, induced through contamination/assimilation, or differences in the evolutionary history of these rocks. Volatile content is clearly one of the parameters which governed crystallization in these rocks. Early crystallization of kaersutite (crystallization orders b and f) is mainly restricted to calcite-bearing rocks. Highly variable Fe^{3+} contents of clinopyroxene phenocrysts furthermore imply that crystallization took place under different T-f_{O_2} conditions, probably ranging from those defined by the QFM buffer to more oxidizing than the NNO buffer.

A comparison between rocks believed to represent melt compositions reveal some chemical contrasts. There is a common negative correlation between MgO, CaO, Sc, Cr, Co, and Ni and the incompatible elements K_2O, Rb, La, Th, etc. (Tables 3, 4, Fig. 5). The more evolved rocks, however, define two separate evolutionary trends. Rocks from Dignes (DI), Viksberget (VI) and sample AU-B1 tend to have higher concentrations of Al_2O_3, Na_2O, and Sr, but lower ones of Sc and Lu at any given evolutionary stage than have rocks from Snaukollen (SN) and

Sønstebyflakene (SØ) (Fig. 5, Table 3). Furthermore, the former group tends to be ne-normative, the latter q-normative.

These compositional contrasts strongly suggest that the two groups of rocks have acquired their present compositions through fractional crystallization dominated by different mineral assemblages. The Dignes (DI) trend imply removal of MgO-CaO-Sc-rich and Al_2O_3-Na_2O-Sr-poor minerals, most likely clinopyroxene (+ olivine?). The phenocryst assemblage ol + plag now found in these rocks consequently

reflect only the latest stage of evolution. The main stage of evolution must have taken place at a higher pressure with an increased field of stability of clinopyroxene relative to plagioclase. The compositional character of the Snaukollen (SN) trend, however, (lower Al_2O_3, Na_2O, Sr, higher Sc) strongly suggests more extensive removal of plagioclase.

Alternatively, one of these trends may reflect contamination, assimilation, or mixing with crustal material.

The relation between crystallization order and
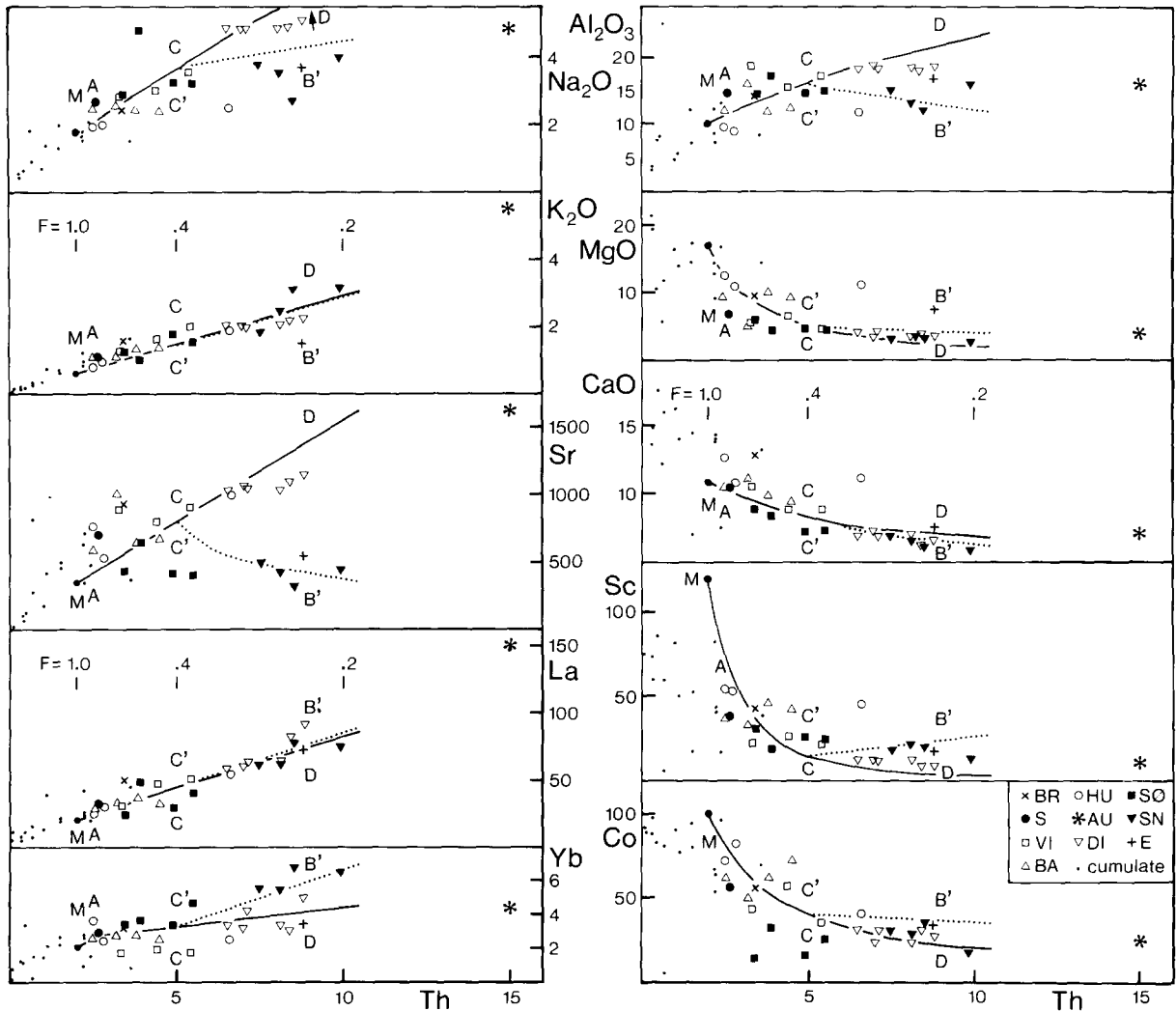
Fig. 5. Selected major and trace elements in Oslo rift gabbros plotted against Th, compared to calculated evolutionary trends. Trend M-A-C-D models crystallization in the lower crust: fractional removal of ol (M-A) followed by $ol_{20}cpx_{80}$ (A-D). Trend C'-B' assumes ascent of magma to the upper crust at stage C, followed by fractional removal of $ol_{30}plag_{70}$. Further explanation is given in the text. Distribution coefficients used to calculate the trends are given in Table 5. F = proportion of liquid. Abbreviations: BR = Brandbukampen, S = Sølvsberget, VI = Viksberget, HU = Husebykollen, AU = Aurenhøgda, DI = Dignes, SØ = Sønstebyflakene, SN = Snaukollen, E = Eiangen.

chemistry is obviously complex and its resolution requires detailed geochemical investigations of individual intrusions. However, even at this preliminary stage certain deductions may be made.

Two observations suggest a two-stage crystallization history:

(1) Rocks with early crystallization of plagioclase (crystallization order c and d) have formed from less mafic melts than have rocks with early crystallization of clinopyroxene (crystallization order a and b). This observation implies that crystallization order is determined by the extent of post-melting processes rather than by the *initial melt chemistry*.

(2) The compositions of some of the rocks (DI, AU-B1) suggest an early stage at some depth dominated by removal of clinopyroxene $\pm$ ol, and a second stage (in situ in the upper crust) with removal of ol + plag.

The question is then if it is theoretically possible to explain the crystallization orders a—d in terms of a two-stage fractionation model assuming one type of primitive melt. The answer is *yes*, and a model for how this could be achieved is illustrated in Fig. 6
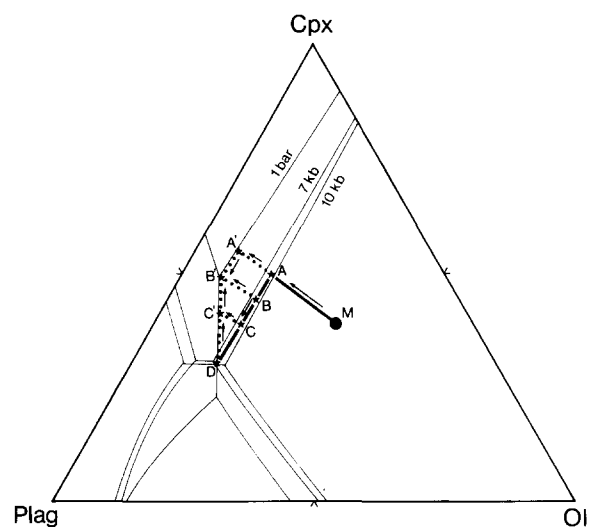
Fig. 6. Variations in crystallization order expected to result from a two-stage fractional crystallization model illustrated in a Fo-Di-An projection (experimental data by Presnall et al., 1978). *M* represents an olivine tholeiitic initial melt. Crystallization starts in the lower crust with removal of olivine followed by clinopyroxene (trend *M-A-B-C-D*). At some stage of evolution residual magma escapes to the upper crust. Depending on the extent of differentiation in the lower crust, crystallization order in the upper crust will be ol—cpx—plag (*A-A'-B'*), ol—plag—cps (*C-C'-B'*) or possibly plag—ol—cpx (*D-B'*).

based on experimental data by Presnall et al. (1978). We assume that an olivine tholeiitic initial melt of composition *M* ascends from its source area in the mantle. In the lower crust this dense mafic magma will lose its buoyancy relative to the side rock (Neumann, 1980). The magma will consequently be retained in the lower crust and crystallize there for a period of time. In our model olivine will be the first mineral on the liquidus, followed by clinopyroxene. The melt composition will, as a result of fractional crystallization in the lower crust, follow a trend such as *M-A-D* in Fig. 6. At irregular intervals melts may escape from the reservoir in the lower crust along newly formed fractures, and ascend to the upper crust. Here a new set of magma chambers is formed where crystallization proceeds. The crystallization order in the upper crust depends on the extent of fractionation in the lower crust. Magmas with a limited degree of crystallization before ascent (compositions in the range *M-A-B*) would at low pressure crystallize olivine followed by clinopyroxene along a path such as *A-A'(-B')*. The olivine-clinopyroxenites and clinopyroxenites of the present study (crystallization order a) belong to this group. Melts with a longer period of residence in the lower crust (compositons *B-D*) would, in the upper crust, crystallize olivine with plagioclase as the second mineral. A typical path would be *C-C'(-B')*. The Dignes (DI) and Snaukollen (SN) trends may represent evolution of the type *M-A-C-D*, and *M-A-C-C'-B'* respectively. Within a limited pressure range about 7 kbar, very extensive crystallization in the lower crust may yield melts (composition *D*) which have plagioclase on the liquidus at low pressure, closely followed by olivine (crystallization order e).

The model has been tested by comparing data on selected major and trace elements with hypothetical evolutionary trends. Distribution coefficients used in the calculations are listed in Table 5, the results are plotted in Fig. 5. The trend *M-A-C-D* represents fractional removal (F = 1 to 0.2) of ol followed by $ol_{20}cpx_{80}$ in the lower crust, the trend *C'-B'* reflects ascent to the upper crust at stage *C* (F = 0.4) followed by removal of the mixture $ol_{30}plag_{70}$ in the upper crust.

The Viksberget (VI), Ballangrudkollen (BA) and Dignes (DI) datapoints fall close to the trend representing crystallization in the lower crust, whereas the Snaukollen (SN) data imply a significant degree of fractional crystallization in the upper crust. The

TABLE 5

Distribution coefficients crystal/melt used to estimate evolutionary trends in Fig. 5. Data from Bender et al. (1978), Drake and Weill (1975), and Irving (1978)

	Ol	Cpx	Plag
Sc	0.3	4.0	0.05
Co	4.0	1.5	0.05
K	0.001	0.002	0.2
Sr	0.003	0.1	2.7
La	0.01	0.15	0.08
Yb	0.03	0.8	0.05
Th	0.001	0.001	0.001
Al_2O_3	0.001	0.6	2.0
MgO	4.6	1.8	0.003
CaO	0.03	1.6	2.0
Na_2O	0.001	0.21	1.0

pyroxenites and olivine-pyroxenites may have formed from melts with only a moderate degree of crystallization in the lower crust, so that they continued to crystallize ol + cpx also after ascent to the upper crust (A'-B' in Fig. 5).

The mildly ne-normative nature of the Dignes (DI) and q-normative nature of the Snaukollen (SN) rocks is compatible with this model. Experimental studies by Kushiro (1968) and Presnall et al. (1978) show that at pressures close to 1 atm crystallization of ol ± cpx ± plag ± en may move a liquid from the field of silica-saturation into the q-normative field. As pressure increases the stability field of ol contracts away from the silica-rich field, and removal of ol ± cpx ± plag ± en from a silica-saturated melt will produce silica-saturated, or, at pressures above about 7 kbar, may even result in mildly silica-undersaturated residual melts.

The crystallization history outlined for these rocks does not rule out the possibility of primary differences in major and trace element compositions of the mantle-derived melts which gave rise to these gabbroic intrusions. It does, however, imply a considerable residence time in the lower or intermediate crust before intrusion into the upper crust where crystallization was completed. Besides the effect of crystallization which is fairly well documented above, the magmas may have been subjected to processes like contamination, assimilation, crystallization in periodically refilled magma chambers, and magma mixing in both the lower and the upper crust. As is shown below, the Sønstebyflakene rocks have been affected by such processes. In Fig. 6 the Sønstebyflakene samples SØ-1, 2, 3 have significantly lower Sr and Co concentrations relative to Th than are expected from the hypothetical trends.

Contamination

The analyzed rocks cover a considerable range in initial $^{87}Sr/^{86}Sr$ ratios (Fig. 3). Significant variations are found both between and within the intrusions. These variations cannot be explained by fractional crystallization alone. It has furthermore been shown that for two of the gabbro intrusions (Dignes and Sønstebyflakene) plots of $^{87}Sr/^{86}Sr$ initial ratios fall close to hypothetical mixing trends (*A-B* and *C-D* in Fig. 5). These data may be explained in terms of mixing between melts derived from different parts of a heterogeneous mantle source, or(/and) contamination of mantle-derived melts during their ascent through the lithosphere. The following discussion is aimed at throwing further light on the relative im-

TABLE 6

Some isotope and trace element data on Permo-Carboniferous Oslo rift gabbros (excluding cumulates) and estimated primary melt (P), compared with estimated means for modern depleted and enriched mid-ocean ridge basalts (MORB), ocean island basalts (OIB) and planetary values. Data from Allègre et al. (1980), Basaltic Volcanism Study Project (1981), Bougault et al. (1980), Sun (1980), and Tarney et al. (1980).

	Oslo gabbros	P	Depleted MORB	Enriched MORB	OIB	Planetary values
Init. $^{87}Sr/^{86}Sr$	0.7037−0.7109	0.7037	0.7024−0.7030	0.7030−0.7035	0.7030−0.7050	0.7045
K/Rb	71−370	220−310	1046	414	436	350
Th/U	3.4 ± 0.4	3.4	2	3	3.5−4.2	4
$(La/Yb)_{EF}$		6	0.7	1.8	12.5	1.0
K (ppm)		5000	1060	1854	9600	120
Sr (ppm)		350	124	180	800	11
La (ppm)		20	3.0	6.3	35	0.315
Th (ppm)		2	0.20	0.55	3.4	0.05

portance of these processes in the genesis of the Oslo rift gabbroic rocks.

In Table 6 selected compositional data for the gabbros of the present study have been compared to values representative of depleted and enriched type mantle-derived magmas, and estimated planetary values. The planetary $^{87}Sr/^{86}Sr$ value of 0.7045 (Allègre et al., 1980) represents zero age, the corresponding value for early Permian time would be about 0.7042. In Figs. 4 and 7 the gabbros are also compared to basement rocks from southeast Norway representing possible sources of contamination.
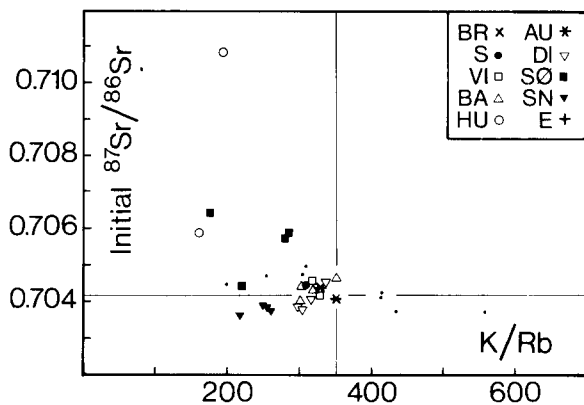
Fig. 7. Variations in K/Rb relative to $^{87}Sr/^{86}Sr$ initial ratios among Oslo rift gabbroic rocks. The lines indicate the K/Rb ratio of the Earth's primitive mantle (Nesbitt and Sun, 1980), and the estimated planetary $^{87}Sr/^{86}Sr$ value in early Permian time. Rocks depleted in Rb and radiogenetic Sr relative to the Earth's primitive mantle plot in the lower right-hand rectangle, enriched rocks in the upper left-hand rectangle. Symbols as in Fig. 5. Small dots are cumulates.

The observed variations in trace element and isotope ratios between the rock types listed in Table 6 are believed to be due to the chemical evolution of the Earth's mantle and crust with time. Small differences have been found to exist in mantle residue-melt bulk distribution coefficients, so that $D_{La}>D_K>D_{Hf}'$ $>D_{Ta}>D_U>D_{Th}>D_{Rb}>D_{Cs}$ (e.g., Sun et al., 1979; Bougault et al., 1980; Sun, 1983). The continuous transfer of incompatible elements from the mantle to the oceanic and continental crust through partial melting have thus left a MORB source region progressively more depleted in Rb and Th than in K and Ta, whereas the continental crust, on the average, is more highly enriched in Th and Rb than in K and Ta. Young N-type MOR basalts consequently have inherited higher K/Rb and Ta/Th ratios from their

source regions than did Archean basalts (Table 5, planetary values). There is furthermore considerable evidence that the lithosphere underneath the continental crust is heterogeneous as the result of processes like underplating, metasomatic enrichment of excluded elements and interaction with magmas (Wass et al., 1980; Weaver and Tarney, 1981).

Melting processes appear to have caused an upward concentration of Cs, Rb, Th, and U, and to a lesser degree, K, also within the continental crust. The REE distribution may not change with depth in the continental crust. As a consequence the upper crust is expected, on the average, to have lower K/Rb, Th/U, (Ta/Th) and higher $^{87}Sr/^{86}Sr$ ratios than has the lower crust (Heier, 1965; Lambert and Heier, 1968; Green et al., 1972; Carter et al., 1978; Tarney et al., 1980).

The low K/Rb and high $^{87}Sr/^{86}Sr$ initial ratios of some of the rocks coupled with highly variable volatile contents probably reflect contamination in the upper crust. The mixing trends of the Sønstebyflakene and Dignes rocks may be modelled by contaminating mantle-derived melts with amphibolite facies (B) Precambrian gneiss and Cambro-Silurian carbonaceus (D) rocks, respectively (Fig. 4). Most affected by contamination are the samples HU-2 and 4, SØ-1, 2, and 3.

It is evident that in the Oslo rift, initial $^{87}Sr/^{86}Sr$ ratios slightly below the 266 Ma planetary value coincide with a wide range in Sr concentrations and a moderate range in K/Rb ratios, including the suggested end-members A and C on the Dignes (DI) and Sønstebyflakene (SØ) mixing trends. However, it has been shown above that considerable trace element differences may be explained by different crystallization histories in the different intrusions. This is illustrated in Fig. 5. The trace element differences between the suggested end-members A and C may thus merely mean that mixing/contamination occurred at a more advanced stage of evolution at Dignes than at Sønstebyflakene. A combination of contamination and fractional crystallization involving removal of plagioclase will, according to DePaolo's calculations (1981), give an evolutionary path which is indistinguishable from that of simple mixing.

The starting points of the hypothetical evolutionary paths in Fig. 5 (and similar ones estimated for other elements) indicate likely element concentrations in the mantle-derived primary magma(s) (P) involved in the formation of the Oslo rift gabbros. Its initial $^{87}Sr/^{86}Sr$ value corresponds to that of the

end-members *A* and *C* in Fig. 4. Selected data on this primary magma is listed in Table 6. In terms of initial Sr ratio the primary magma is depleted, whereas its incompatible element concentrations and ratios fall between values characteristic of enriched mid-ocean ridge and ocean island basalts. The origin of the primary magma(s) is thus not obvious. However, the system of NW-SE-trending strike-slip faults accompanied by N-S-trending rifts and associated magmatic activity in the Northwest Europe in Upper Carboniferous-Permian time, may well have been initiated by late Hercynian movements (rotation of the Gondwana plate relative to the Laurasia plate). (This problem is discussed in some detail in a separate paper). It is therefore more likely that magmatism in the Oslo rift reflect melting associated with rupture of the lithosphere (melting of the lower lithosphere or admission of asthenospheric melts, i.e. a depleted source), than the activity of any underlying mantle plume. The apparent inconsistency between initial Sr isotope and incompatible element data may reflect the effect of processes like zone refining or contamination in the lower crust.

Summary and conclusions

(1) The small mafic intrusions in the Oslo rift consist of a variety of rock types ranging from pyroxenite and gabbro to monzonite and anorthosite, and comprise both cumulates and rocks believed to represent melt compositions. The rocks formed from mildly silica-undersaturated to mildly silica-oversaturated melts with Mg-values $\leqslant 0.66$, strongly enriched in incompatible elements, and in light relative to heavy REE.

(2) Rb-Sr isotope data define a whole rock age of 265 ± 11 Ma for the Snaukollen and a mineral age of 266 ± 5 Ma for the Dignes intrusion. These ages imply that the mafic intrusions were emplaced at a relatively late stage of the rifting episode.

(3) The rocks exhibit a variety of phenocryst/cumulus crystal assemblages including ol + cpx; ol + cpx + plag; ol + plag. Ti-rich amphibole occasionally represents an early phase.

(4) The implied differences in crystallization orders, and the compositional relations found to exist among the majority of the rocks are compatible with a two-stage crystallization history: An early stage at depth in the crust is dominated by removal of ol + cpx. The liquidus assemblage at the second stage, that is after ascent to the upper crust, is dependent on the extent of crystallization in the lower crust: low extent gives ol + cpx, high extent gives ol + plag.

(5) Initial $^{87}Sr/^{86}Sr$ ratios (assuming an age of 266 Ma) range from 0.70367 ± 11 to 0.71083 ± 9, implying the influence of both mantle-derived and crustal components.

(6) Estimated Sr initial ratio for the mantle-derived primary magma(s) involved in the formation of the gabbros is below the planetary value of 0.7042 for early Permian time, whereas concentrations of incompatible elements are between those typical of magmas derived from depleted and enriched type sources. It is concluded that the primary magma(s) is derived from the lower lithosphere or asthenosphere, but may have been somewhat enriched in incompatible elements through zone refining or interaction with the Rb-depleted lower crust. Magmatism in the Oslo rift thus appears to reflect melting of a depleted source rather than an underlying mantle plume.

(7) The high $^{87}Sr/^{86}Sr$ initial ratios, low K/Rb ratios and low Sr concentrations of some of the rocks are compatible with in situ contamination of the mantle-derived magma(s) by amphibolite facies, Precambrian gneisses and Cambro-Silurian carbonaceous rocks. Most affected are some of the samples from Husebykollen (H) and Sønstebyflakene (SØ).

(8) The rocks have crystallized under different partial pressures with respect to CO_2, and T-f_{O_2} conditions probably ranging from those defined by the QFM buffer to more oxidizing than the NNO buffer. The most oxidizing conditions are found for the most highly contaminated rocks, a fact which suggests that volatiles may have been induced in the crust. However, also chemical differences among the primary melts, reflecting melting of a heterogeneous mantle source, may exist. Such differences are difficult to identify in rocks which have gone through complex and extensive post-melting processes, such as is the case with the Oslo rift gabbroic rocks.

Acknowledgements

58

References

Allègre, C.J., Brévart, O., Dupré, B. and Minster, J.-F., 1980. Istopic and chemical effects produced in a continuously differentiating convecting Earth mantle. Philos. Trans. R. Soc. London, Ser. A, 297: 447–477.

Barth, T.F.W., 1945. Studies on the igneous rock complex of the Oslo Region, II. Systematic petrography on the plutonic rocks. Skr. Nor. Vidensk. Akad. Oslo, 1: Mat.-Naturv. Kl. 1944, 9: 104 pp.

Basaltic Volcanism Study Project, 1981. Basaltic Volcanism on the Terrestrial Planets. Pergamon Press, New York, N.Y., 1286 pp.

Bender, J.F., Hodges, F.N. and Bence, A.E., 1978. Petrogenesis of basalts from the Project FAMOUS area: experimental study from 0 to 15 kbars. Earth Planet. Sci. Lett., 41: 277–302.

Bougault, H., Joron, J.L. and Treuil, M., 1980. The primordial chrondritic nature and large-scale heterogeneities in the mantle: evidence from high and low partition coefficients in oceanic basalts. Philos. Trans. R. Soc. London, Ser. A, 297: 203–213.

Brøgger, W.C., 1894. The basic eruptive rocks of Gran. Geol. Soc. London Q. J., 50: 15–38.

Brøgger, W.C., 1931. Die Eruptivgesteine des Oslogebietes, V. Der grosse Hurumvulkan. Skr. Nor. Vidensk. Akad. Oslo, 1: Mat.-Naturv. Kl. 1930, 6: 146 pp.

Brøgger, W.C., 1933a. Die Eruptivgesteine des Oslogebietes, VII. Die chemische Zusammensetzung der Eruptivgesteine des Oslogebietes. Skr. Nor. Vidensk. Akad. Oslo, 1: Mat.-Naturv. Kl. 1933, 1: 147 pp.

Brøgger, W.C., 1933b. Essexitrekkens erupsjoner. Nor. Geol. Unders., 138: 103 pp.

Brunfelt, A.O. and Steinnes, E., 1969. Instrumental activation analysis of silicate rocks with epithermal neutrons. Anal. Chim. Acta, 48: 13–24.

Cameron, M. and Papike, J.J., 1981. Structural and chemical variations in pyroxenes. Am. Mineral., 66: 1–50.

Carter, S.R., Evensen, N.M., Hamilton, P.J. and O'Nions, R.K., 1978. Neodynium and strontium isotope evidence for crustal contamination of continental volcanics. Science, 202: 743–746.

DePaolo, D.J., 1981. Trace element and isotopic effects of combined wallrock assimilation and fractional crystallization. Earth Planet. Sci. Lett., 53: 189–202.

Dons, J.A., 1952. Studies on the igneous rock complex of the Oslo Region, XI. Compound volcanic neck, igneous dykes, and fault zone in the Ullern-Husebyåsen area, Oslo. Skr. Nor. Vidensk. Akad. Oslo, 1: Mat.-Naturv. Kl. 1952, 2: 96 pp.

Drake, M.J. and Weill, D.F., 1975. Partition of Sr, Ba, Ca, Y, Eu^{2+}, Eu^{3+}, and other REE between plagioclase feldspar

and magmatic liquid: an experimental study. Geochim. Cosmochim. Acta, 39: 689–712.

Faure, G., 1977. The Principles of Isotope Geology. John Wiley, New York, N.Y.

Finstad, K.G., 1972. En undersøkelse av utvalgte edelmetaller og sjeldne jordartselementer i noen norske, hovedsakelig basiske og ultrabasiske bergarter. Thesis (unpublished), University of Oslo, Oslo, 113 pp.

Gordon, G.C., Randle, K., Goles, G.G., Corliss, J.B., Beeson, M. H. and Oxley, S.S., 1968. Instrumental activation analysis of standard rocks with high-resolution gamma-ray detectors. Geochim. Cosmochim. Acta, 32: 369–396.

Green, T.H., Brunfelt, A.O. and Heier, K.S., 1972. Rare-earth element distribution and K/Rb ratios in granulites, mangerites and anorthosites, Lofoten-Vesteraalen, Norway. Geochim. Cosmochim. Acta, 36: 241–257.

Hanson, G.N. and Langmuir, C.H., 1978. Modelling of major elements in mantle-melt systems using trace element approaches. Geochim. Cosmochim. Acta, 42: 725–741.

Harnik, A.B., 1969. Strukturelle Zustände in den Anorthoklasen der Rhombenporphyre des Oslogebietes. Schweiz. Mineral. Petrogr. Mitt., 49: 509–567.

Heier, K.S., 1965. Metamorphism and the chemical differentiation of the crust. Geol. Fören. Stockholm Förh., 87: 249–256.

Helz, R.T., 1973. Phase relations of basalts in their melting range at P_{H_2O} = 5 kb as a function of oxygen fugacity, I. Mafic phases. J. Petrol., 14: 249–302.

Huckenholz, H.G., 1973. The origin of fassaitic augite in the alkali basalt suite of the Hocheifel area, Western Germany. Contrib. Mineral. Petrol., 40: 315–326.

Irvine, T.N., 1982. Terminology for layered intrusions. J. Petrol., 23: 127–162.

Irving, A.J., 1978. A review of experimental studies of crystal/liquid trace element partitioning. Geochim. Cosmochim. Acta, 42: 743–770.

Jacobsen, S.B. and Heier, K.S., 1978. Rb-Sr isotope systematics in metamorphic rocks, Kongsberg sector, South Norway. Lithos, 11: 257–276.

Kushiro, I., 1968. Compositions of magmas formed by partial zone melting of the earth's upper mantle. J. Geophys. Res., 73: 619–634.

Lambert, I.B. and Heier, K.S., 1968. Geochemical investigations of deep-seated rocks in the Australian shield. Lithos, 1: 30–53.

Larsen, B.T., 1978. Krokskogen lava area. Nor. Geol. Unders., 337: 143–162.

Larsen, B.T., Ramberg, I.B. and Schou Jensen, E., 1978. Central part of the Oslo fjord. Nor. Geol. Unders., 337: 105–124.

McCulloh, T.H., 1952. Studies on the igneous rock complex of the Oslo Region, X. Geology of the Grefsen-Grorud area, Oslo, Norway. Skr. Nor. Vidsk. Akad. Oslo, 1: Mat.-Naturv. Kl. 1952, 1: 50 pp.

Mysen, B.O. and Kushiro, I., 1977. Compositional variation of coexisting phases with degree of melting of peridotite in the upper mantle. Am. Mineral., 62: 843–865.

Navrotsky, A., 1978. Thermodynamics of element partitioning: (1) systematics of transition metals in crystalline and

molten silicates and (2) defect chemistry and "the Henry's law problem". Geochim. Cosmochim. Acta, 42: 887–902.

Nesbitt, R.W. and Sun, S.-S., 1980. Geochemical features of some Archaean and post-Archaean high-magnesian-low-alkali liquids. Philos. Trans. R. Soc. London, Ser. A, 297: 365–381.

Neumann, E.-R., 1980. Petrogenesis of the Oslo Region larvikites and associated rocks. J. Petrol., 21: 498–531.

Nielsen, R.L. and Drake, M.J., 1979. Pyroxene-melt equilibria. Geochim. Cosmochim. Acta, 43: 1259–1272.

Oftedahl, C., 1952. Studies on the igenous rock complex of the Oslo Region, XII. The lavas. Skr. Nor. Vidensk. Akad. Oslo, 1: Mat.-Naturv. Kl. 1952, 3: 64 pp.

Oftedahl, C., 1953. Studies on the igneous rock complex of the Oslo Region, XIII. The cauldrons. Skr. Nor. Vidensk. Akad. Oslo, 1: Mat.-Naturv. Kl. 1953, 3: 108 pp.

Onuma, K., 1983. Effect of oxygen fugacity on fassaitic pyroxene. J. Fac. Sci. Hokkaido Univ., Ser. IV, 20: 185–194.

Papike, J.J. and White, C., 1979. Pyroxenes from planetary basalts: characterization of "other" than quadrilateral components. Geophys. Res. Lett., 6: 913–916.

Presnall, D.C., Dixon, S.A., Dixon, J.B., O'Donnell, T.H., Brenner, N.L., Schrock, R.L. and Dycus, D.W., 1978. Liquidus phase relations on the join diopside-forsterite-anorthite from 1 atm. to 20 kbar: their bearing on the generation and crystallization of basaltic magma. Contrib. Mineral. Petrol., 66: 203–220.

Ramberg, I.B., 1970. Vulkanpluggene ved Vestby. Nytt fra Oslofelt-gruppen 1, 1970: 26–40.

Ramberg, I.B., 1976. Gravity interpretation of the Oslo Graben and associated igneous rocks. Nor. Geol. Unders., 325: 194 pp.

Ramberg, I.B. and Larsen, B.T., 1978. Tectonomagmatic evolution. In: J.A. Dons and B.T. Larsen (Editors), The Oslo Paleorift. A Review and Guide to Excursions. Nor. Geol. Unders., 337: 55–73.

Segalstad, T.V., 1979. Petrology of the Skien basaltic rocks, southwestern Oslo Region, Norway. Lithos, 12: 221–239.

Steinlein, O.A., 1981. En petrologisk og geokjemisk undersøkelse av lagdelte, gabbroide vulkanplugger i Hurum Oslo-graben. Thesis (unpublished), University of Oslo, Oslo, 93 pp.

Streckeisen, A., 1976. To each plutonic rock its proper name. Earth Sci. Rev., 12: 1–33.

Sun, S.-S., 1980. Lead isotopic study of young volcanic rocks from mid-ocean ridges, ocean islands and island arcs. Philos. Trans. R. Soc. London, Ser. A, 297: 409–445.

Sun, S.-S., 1983. Geochemical characteristics of Archaean ultramafic and mafic volcanic rocks: implications for mantle composition and evolution. In: IGCP Project 92: Archean Geochemistry. Springer-Verlag, Berlin (in press).

Sun, S.-S., Nesbitt, R.W. and Sharaskin, A.Ya., 1979. Geochemical character of mid-ocean ridge basalts. Earth Planet. Sci. Lett., 44: 111–138.

Sundvoll, B., 1978a. Rb/Sr-relationship in the Oslo igneous rocks. In: E.-R. Neumann and I.B. Ramberg (Editors), Petrology and Geochemistry of Continental Rifts. D. Reidel, Dordrecht, pp. 181–184.

Sundvoll, B., 1978b. Isotope- and trace-element chemistry. In: J.A. Dons and B.T. Larsen (Editors), The Oslo Paleorift. A Review and Guide to Excursions. Nor. Geol. Unders., 337: 35–40.

Tarney, J., Wood, D.A., Sanders, A.D., Cann, J.R. and Varet, J., 1980. Nature of mantle heterogeneity in the North Atlantic: evidence from deep sea drilling. Philos. Trans. R. Soc. London, Ser. A, 297: 179–202.

Wass, S.Y., Henderson, P. and Elliot, C.J., 1980. Chemical heterogeneity and metasomatism in the upper mantle: evidence from rare earth and other elements in apatite-rich xenoliths in basaltic rocks from eastern Australia. Philos. Trans. R. Soc. London, Ser. A, 297: 333–346.

Weaver, B.L. and Tarney, J., 1981. The Scourie dyke suite: petrogenesis and geochemical nature of the Proterozoic subcontinental mantle. Contrib. Mineral. Petrol., 78: 175–188.

Weigand, P.M., 1975. Studies on the igneous rock complex of the Oslo Region, XXIV. Geochemistry of the Oslo basaltic rocks. Skr. Nor. Vidensk. Akad. Oslo, 1: Mat.-Naturv. Kl. Ny Ser., 34: 38 pp.